Phage-display selected cyclic peptide inhibitors of kallikrein-related peptidases 5 and 7 and their in vivo delivery to skin

Patrick Gonschorek[1], Alessandro Zorzi[1], Tamara Maric[1], Mathilde Le Jeune[1], Mischa Schüttel[1], Mathilde Montagnon[1], Rebeca Gómez-Ojea[1], Denis Patrick Vollmar[1], Chantal Whitfield[1], Luc Reymond[2], Vanessa Carle[1], Hitesh Verma[1], Oliver Schilling[3], Alain Hovnanian[4] and Christian Heinis[1]*

[1]Institute of Chemical Sciences and Engineering, School of Basic Sciences, Ecole Polytechnique Fédérale de Lausanne (EPFL), CH-1015 Lausanne, Switzerland

[2]Biomolecular Screening Facility, Swiss Federal Institute of Technology Lausanne (EPFL), CH-1015 Lausanne, Switzerland

[3]Institute for Surgical Pathology, Medical Center, Faculty of Medicine, University of Freiburg, Freiburg, Germany

[4]INSERM UMR1163, Imagine Institute, University of Paris, Paris, France; Department of Genetics, Necker Hospital for Sick Children (AP-HP), Paris, France

*Correspondence should be addressed to Christian Heinis (christian.heinis@epfl.ch)

Keywords: cyclic peptide, KLK5, KLK7, Netherton syndrome, phage display, protease inhibitor, tissue kallikrein-related peptidase

ABSTRACT

Kallikrein-related peptidases 5 (KLK5) and 7 (KLK7) are serine proteases with homeostatic functions in the epidermis that play a critical role in Netherton Syndrome (NS), a rare yet life-threatening genetic disorder that currently lacks specific treatment. Previous research suggests that controlling KLKs could lead to the development of NS therapies, but existing synthetic inhibitors have limitations. Herein, we used phage display to screen libraries comprising more than 100 billion different cyclic peptides and found selective, high-affinity inhibitors of KLK5 (K_i=2.2±0.1 nM) and KLK7 (K_i=16±4 nM). By eliminating protease-prone sites and conjugating the inhibitors to an albumin-binding peptide, we enhanced inhibitor stability and prolonged the elimination half-life to around five hours in mice. In tissue sections taken from mice, fluorescently labeled peptide was detected in the epidermis, suggesting that the inhibitors can reach the KLKs upon systemic delivery and should be suited to control deregulated protease activity in NS.

INTRODUCTION

Kallikrein-related peptidases 5 and 7 are serine proteases that play important roles in the homeostasis of skin and desquamation. Dysregulation of these proteases causes the rare disease Netherton syndrome (NS) and is also implicated in more common skin disorders such as rosacea, atopic dermatitis, and psoriasis. The two proteases are expressed as inactive zymogens by cells of the stratum granulosum and secreted into the extracellular space of the stratum corneum—the two outermost layers of the skin, and become active only after their pro-domain is cleaved by an already active protease. KLK5 can auto-activate itself and subsequently cleave the pro-domains of pro-KLK7, pro-KLK8, and pro-KLK14 to activate these proteases. Active KLK5 and KLK7 cleave corneocyte-connecting proteins, such as desmoglein 1, desmocollin 1, and corneodesmosin, leading to desquamation. Via a second pathway, KLK5 and KLK14 cleave and thereby trigger protease-activated receptor 2 (PAR2), which can cause inflammation. Active KLK14 can activate KLK5 again, amplifying the activation of the cascade in a positive feedback loop. KLKs are regulated by lympho-epithelial Kazal-type related inhibitor (LEKTI), which is encoded by serine peptidase inhibitor Kazal-type 5 (*SPINK5*).[1]

Loss of function mutations in the *SPINK5* gene cause NS, a rare yet severe skin disease that occurs with an autosomal recessive inheritance in 1:200,000 newborns.[2] More than 70 mutations in *SPINK5*, such as insertions, deletions, or substitutions, have been reported, a majority of which lead to premature stop codons. The disease is characterized by severe skin inflammation and excessive skin scaling (desquamation) that result from insufficient KLK regulation by LEKTI. PAR2 activation by KLK5 and KLK14 leads to skin inflammation, while cleavage of cell-cell connecting desmosomes by KLK5 and KLK7 cause desquamation. This results in a profound skin barrier defect, which promotes infections and dehydration, both of which are life threatening complications in newborns and in infants. Even though the condition often partially improves with age and patients have a normal life expectancy, their quality of life is

severely impaired by persistent itchiness with chronic or acute flares of severe skin inflammation.[3] Individual or combined KLK5 and KLK7 knock-out in LEKTI-deficient newborn mice rescued a number of NS-like pathological manifestations to different extents[4,5] and suggested that inhibition of these proteases could be sufficient to reach therapeutic effects in NS patients.

Currently, there is no specific treatment available for NS. Treatment approaches that are being tested include intravenous immunoglobulin (IVIG) therapy and several biologics including anti-TNFα treatment, anti-IL17 (secukinumab, ixekizumab), anti-IL4R/IL13R (dupilumab), anti-IL12/23 (ustekinumab).[3] However, neither provides specific treatment, which would ideally restore or replace LEKTI function. Several protein-, peptide-, and small–molecule-based inhibitors of KLK5 and KLK7 have been developed as described in the following.[3,6,7] Fragments or individual domains of LEKTI inhibit the two KLKs, with the most potent fragment, D8-D11, inhibiting KLK5 and KLK7 with K_is of 3.7 nM and 34.8 nM, respectively. The most potent single domain of LEKTI is D5, which inhibits KLK5 and KLK7 with K_is of 32.8 nM and 77.2 nM, respectively.[8] Several groups have generated peptide-based KLK5 and KLK7 inhibitors by altering the specificity loop of sunflower trypsin inhibitor (SFTI-1).[9–13] The most potent SFTI-1-based KLK5 and KLK7 inhibitors have K_is of 0.34 nM and 0.14 nM, respectively.[11,13] A potent KLK7 inhibitor was also developed based on a cyclic depsipeptide, but its intricate, natural–product-based structure makes its preparation rather complex.[14] A range of small molecule inhibitors were identified, with the best KLK5 inhibitors having medium nM potency[15–20] and the best KLK7 inhibitors having low nM potency.[21] A challenge with small molecule inhibitors has been the achievement of sufficient selectivity over the various trypsin and chymotrypsin-like serine proteases present in humans, several of which have important functions.

Herein, we have used *in vitro* evolution to develop high affinity inhibitors of KLK5 and KLK7 based on simple cyclic peptide structures that are chemically easily accessible

and should facilitate the development of an NS therapy. We reasoned that sampling billions of cyclic peptides with various random sequences would lead to the identification of structures that fit perfectly into the active sites of the two KLKs and therefore bind with highest possible affinity. To achieve this, we screened the largest phage display peptide library developed to date that contained > 100 billion cyclic and bicyclic peptides. As described in the following, the screens led to the identification of potent KLK5 and KLK7 inhibitors that could be shrank in size, improved in stability and pharmacokinetic properties, and were found to concentrate exactly where the target proteins were located in the epidermis, after intravenous injection in mice.

RESULTS AND DISCUSSION

Phage display selection of inhibitors of KLK5 and KLK7

We used phage display to screen a library of around 2.8×10^{10} random peptides of the format $XC(X)_mC(X)_nC(X)_oCX$ (where C = cysteine, X = any random amino acid, m + n + o = 12), which was recently developed in our lab (Figure 1a).[22] Prior to the affinity selections, we formed bridged peptides by reacting the phage-displayed peptides with bis-electrophiles that connect cysteine pairs. This generated the three possible cyclic peptide configurations shown on the right in Figure 1a for each peptide in the library. The first peptide configuration contains two monocyclic peptides spaced by a random peptide linker (dumbbell shape). The second and third configurations are bicyclic peptides. Since the applied library is currently the largest peptide phage display library to our knowledge, we expected it to be an ideal source for KLK inhibitor identification. We cyclized approximately 2.8×10^{10} random peptides in parallel reactions with 2,6-bis(bromomethyl)pyridine (BBMP) and 1,3-dibromoacetone (DBA) (Figure 1a). This generated > 100 billion different monocyclic peptides (2 cyclization reagents × 2 monocyclic peptides × 2.8×10^{10}) and > 100 billion bicyclic peptides (2 cyclization reagents × 2 bicyclic peptide formats × 2.8×10^{10}).

To generate the proteins for screening, we expressed human KLK5 and KLK7 in mammalian cell suspension cultures as zymogens and with signal sequences for secretion into the supernatant (Figure S1a and S1b). For KLK5, we ensured auto-activation of the zymogen by expressing the catalytic domain with the native pro-domain. For KLK7, we tried two different strategies for expression and zymogen activation, with the more effective strategy involving expression of the catalytic domain with an artificial pro-domain that ended with the motif Tyr-Leu. This motif was recognized by KLK7 as a substrate, leading to partial auto-activation of the zymogen. We purified the proteases via C-terminal histidine tags and assessed zymogen activation with both SDS-PAGE and activity assays, using a fluorogenic substrate for KLK5 and a recently reported chromogenic substrate for KLK7[11] that we synthesized

in-house (Figure S1c-e). We biotinylated the two proteases via lysine side chains for immobilization on magnetic streptavidin or neutravidin beads. Screening involved three rounds of selections, altering the beads in between rounds to prevent enrichment of streptavidin or neutravidin binders, and using 10, 5, and 2.5 μg of KLK5 and KLK7 in rounds 1 to 3.

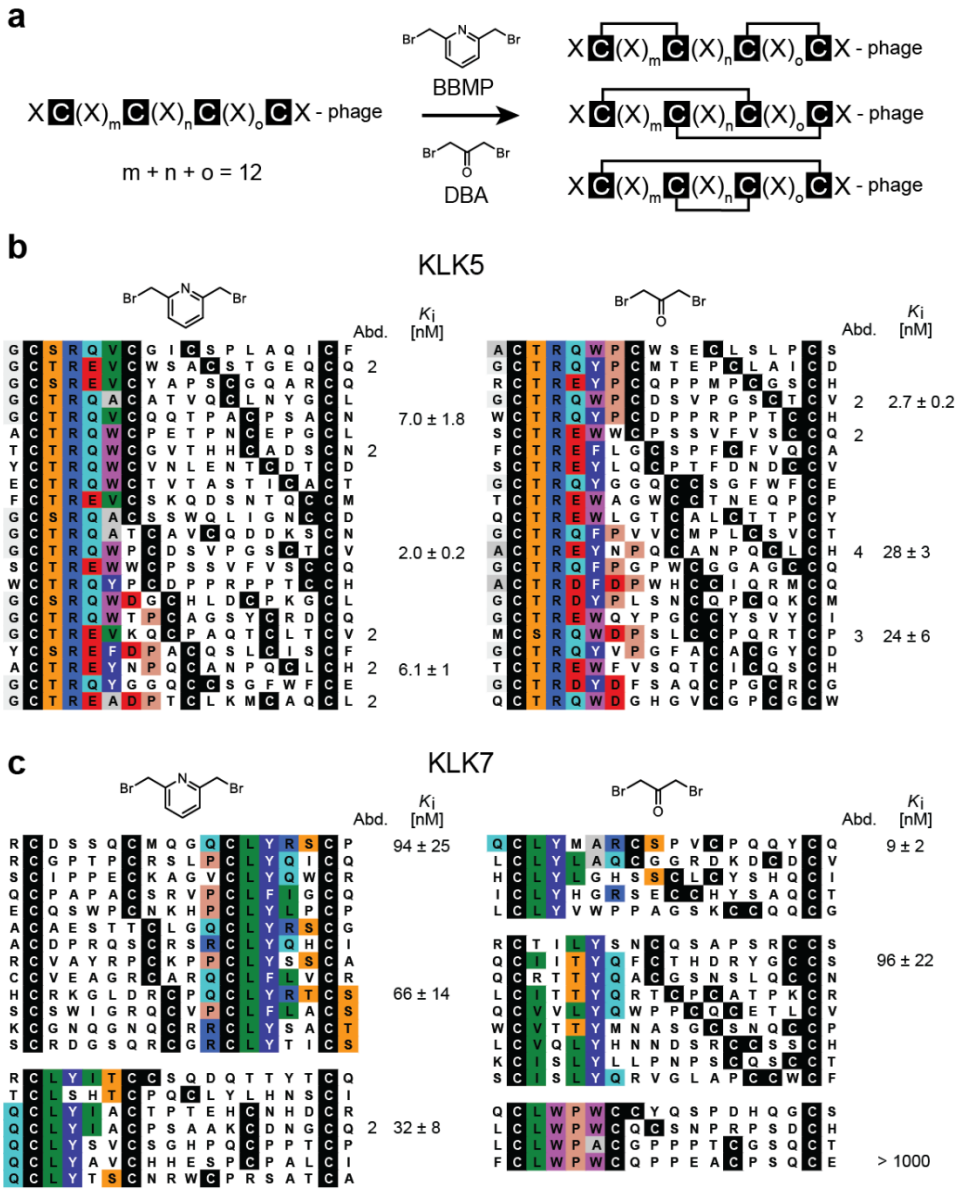

Figure 1. Phage display selection of (bi)cyclic peptides against KLK5 and KLK7. (a) Format of peptide phage display library, with X representing random amino acids and C representing cysteine. The cyclization reagents BBMP and DBA bridge two cysteine pairs in each peptide to yield three different double-bridged peptide formats. (b, c) Peptides enriched

after three rounds of phage selection against (b) human KLK5 and (c) human KLK7. Peptides sharing a consensus sequence are grouped, and similar amino acids are highlighted using colors. Abundance is indicated for peptides found more than once. Inhibition constants are indicated for peptides that were synthesized. Mean values and SDs of three independent measurements are shown.

Sequencing of the isolated phage revealed strong similarities among peptides enriched to KLK5 (Figure 1c) and peptides enriched to KLK7 (Figure 1d). The consensus sequences covered 3–5 amino acids and were flanked by cysteines on both sides, suggesting that the peptides bound as monocycles in the "dumbbell" configuration. Peptides isolated against KLK5 shared a common motif of the sequence $^{T}/_{S}R^{Q}/_{E}$ following the first Cys. The Arg found in all peptides is most likely binding to the S1 sub-site of the substrate-binding region of the trypsin-like serine protease that is known to accommodate positively charged residues. In peptides cyclized with the linker BBMP, the $^{T}/_{S}R^{Q}/_{E}$ motif was often followed by Val or Trp ($^{T}/_{S}R^{Q}/_{E}{}^{V}/_{W}$), and in peptides cyclized with the linker DBA, the motif was followed by Trp or Tyr and then by Pro ($^{T}/_{S}R^{Q}/_{E}{}^{W}/_{Y}P$). Most peptides enriched against KLK7 shared the short core motif LY that followed the first or third Cys. The Tyr found in this motif is most likely binding to the S1 sub-site of the substrate binding region of the chymotrypsin-like serine protease that is known to accommodate large, hydrophobic residues. In many peptides, this motif was extended, for example, with Gln preceding the Cys (Q<u>C</u>LY). Given the sequence similarities of the inhibitors to KLK5 and KLK7 substrates, there is the possibility that they are cleaved after Arg and Tyr, respectively. We did not observe any loss of inhibitory activity when incubating the inhibitors with the proteases, indicating that they are either not cleaved, or that the linearized peptides remain active as inhibitors.

Bicyclic peptides inhibit KLK5 and KLK7 with nanomolar affinity

To assess the inhibition of these identified peptides, we synthesized representative linear peptides of each consensus sequence, cyclized them with linker that was used

in the selection, and purified them by HPLC. Where possible, we chromatographically separated the three isomers that form due to disulfide bridging (Figure 1a). Figures 1b and 1c show the K_is of the most active isomers for each peptide. The KLK5 peptides inhibited the protease with inhibition constants in the nanomolar range, several with single-digit nM K_is (Figure 1b and Figure S2). Similarly, the KLK7 peptides inhibited the protease with nanomolar affinities, though with slightly weaker potency overall. The best K_is for the cyclic peptide KLK7 inhibitors were approximately 10 nM (Figure 1c and Figure S2). Judging based on the binding affinity of LEKTI to its target proteins, it is expected that an inhibitor in the single-digit nanomolar range will be sufficient for modulating KLK5 and KLK7 activity in diseases like NS.

Given that the isolated peptides were most likely binding the KLKs as monocycles, we next synthesized only the regions containing the consensus motifs together with the flanking cysteines. We included additional amino acids adjacent to the cysteines only if they appeared important based on the consensus sequence (Figure 2a and 2b). The monocyclic peptides inhibited the KLKs with similar potencies as the enriched peptides, confirming that the phage-selected bicyclic peptides were interacting with the targets mainly via one of the two peptide loops. The best monocyclic KLK5 inhibitor had a K_i of 1.4 ± 0.1 nM (Figure 2a and Figure S2), and the best KLK7 inhibitor had a K_i of 8.8 ± 1.2 nM (Figure 2a and Figure S2). These affinities were slightly weaker than the best inhibitors reported,[11,13] but synthetically they are easier to access, facilitating further development, conjugation or production. The finding that short monocyclic peptides were suited for binding suggested that it could be an attractive strategy to directly screen monocyclic peptide libraries against the two targets. Using phage display libraries of shorter peptides would offer the advantage that all possible peptide sequences could be represented in a library.

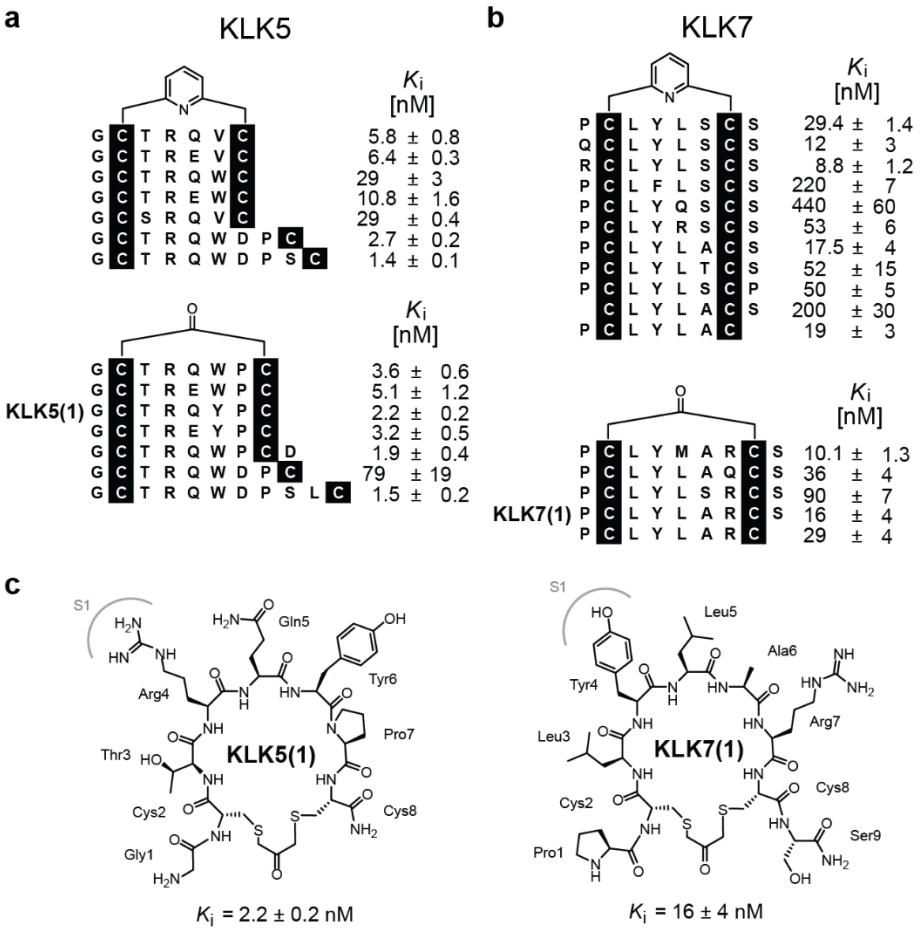

Figure 2. Inhibition activity of monocyclic peptides. (a, b) Sequences and inhibitory constants (K_i) of cyclic peptides for (a) KLK5 and (b) KLK7. Mean values of three independent measurements are shown and SDs are indicated. (c) Chemical structures of KLK5(1) (KLK5 inhibitor) and KLK7(1) (KLK7 inhibitor) chosen as leads for further development.

We next estimated the specificity level of one of the monocyclic peptide KLK5 inhibitors (KLK5(1); Figure 2c) by testing the inhibition of seven trypsin-like serine proteases that have the same fold as KLK5 and similar substrate specificity. Most of the proteases were not inhibited at all, and the two that showed inhibition had constants in the high micromolar range, corresponding to a greater than 4000-fold target selectivity (Figure S3). This matches with our previous work on cyclic and bicyclic peptide inhibitors developed by phage display to other serine proteases, such as plasma kallikrein, urokinase-type plasminogen activator (uPA), coagulation factor XI or coagulation factor XII. In all these examples, a high target selectivity was maintained, even in cases

where the active sites were highly similar.[23,24] While an in depth specificity profiling with a much broader panel of serine proteases will be required to exclude inhibition of other proteases, we concluded that the inhibitors most likely have a safe selectivity profile.

Structure-activity relationship study and affinity improvement by unnatural amino acids

To study the structure-activity relationship (SAR) of the amino acids and to improve the binding affinity of the less active KLK7 inhibitor, we synthesized variants of the best KLK5 and KLK7 inhibitors. As a starting point, we chose two relatively short peptides, KLK5(1) (K_i of 2.2 ± 0.2 nM) and KLK7(1) (K_i of 16 ± 4 nM) (Figure 2c), that inhibited KLK5 and KLK7, respectively. Of the 32 variants of KLK5(1), most showed a much lower activity and only a few had a conserved or slightly improved K_i, with all improvements smaller than a factor of two (Figure 3a, Figure S4 and S5a). The SAR study showed that most of the residues in peptide KLK5(1) were essential and could barely be altered, but Gln5 and Tyr6 were the least important. For KLK7(1), we synthesized variants of the peptide not containing the C-terminal Ser (K_i for KLK7 = 29 ± 4 nM). Of the 26 variants of KLK7(1), the substitution of Leu5 to norleucine (Nle) improved the inhibition constant around 4-fold (K_i = 7 ± 0.7 nM, KLK7(2)) (Figure 3b, Figure S4, and S5b). The SAR study with KLK7(1) showed that all amino acids in this peptide were essential, and the most important ones were Leu3 and Tyr4, which form the LY signature of the consensus sequences. This result suggests that the peptides interact via several amino acids and many molecular contacts with the KLKs, and thus are highly specific inhibitors.

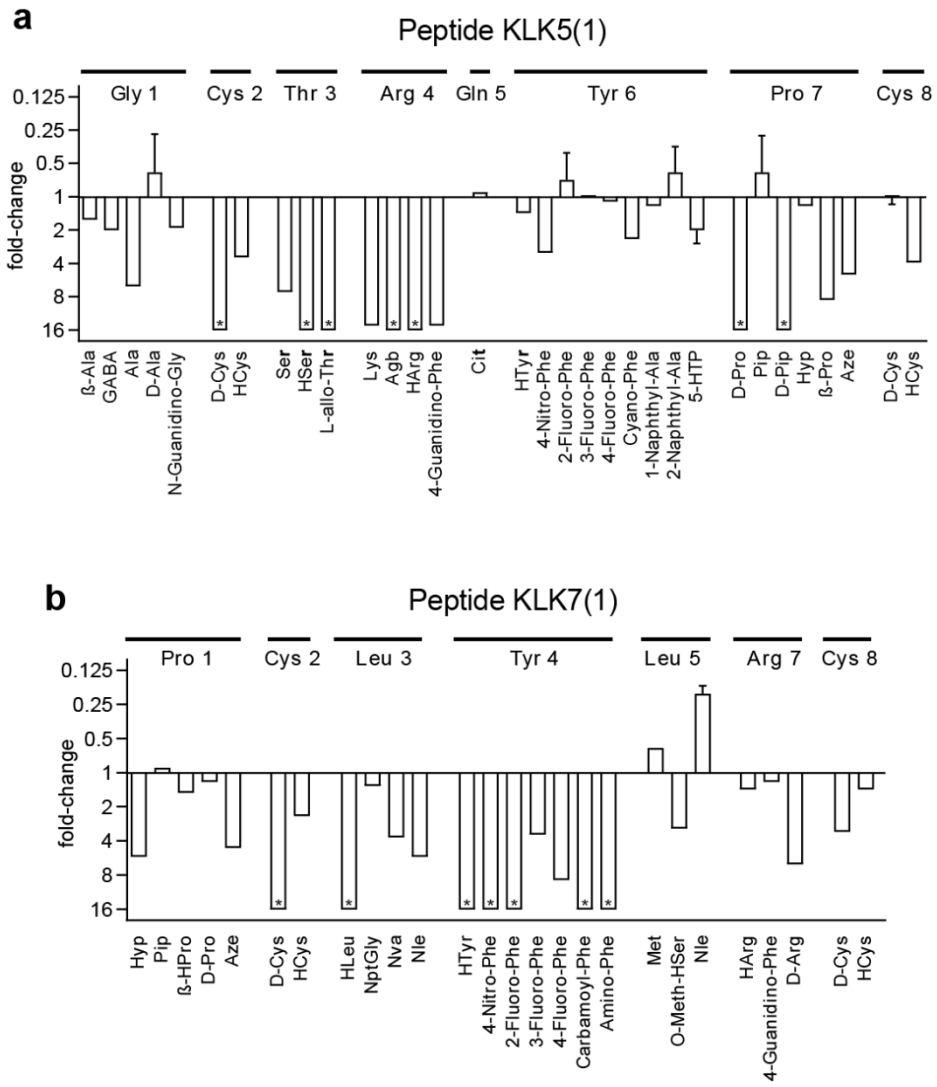

Figure 3. Structure-activity relationship analysis and affinity improvement by substitutions to unnatural amino acids. (a, b) Amino acid substitutions in (a) KLK5-inhibiting peptide KLK5(1) and (b) KLK7-inhibiting peptide KLK7(1). Changes to the K_i are shown, with values less than one (above the x-axis) indicating improvements. KLK7(1) and its mutants were synthesized without the C-terminal serine. Asterisks (*) indicate K_i values that were more than 16-fold worse. For peptides showing improved or unchanged activity, the measurement of the K_i values was repeated in two additional experiments, and mean values and SDs are indicated.

Tethering of KLK inhibitors to albumin retains their activity

While topical delivery of cyclic peptide KLK inhibitors could be a viable option for the treatment of NS due to the permeable skin of patients, we focused in this study on intravenous delivery, which would offer the advantage of a systemic treatment and thus

inhibition of the KLKs throughout the body. Most systemically administered peptides are cleared from the blood stream within minutes or hours by proteolytic degradation and/or renal filtration, preventing extravasation and diffusion into the skin and therefore thwarting KLK inhibition. An established strategy to prolong the circulation time of peptides is based on conjugating them to fatty acids or other ligands of albumin.[25] Tethering the peptides to the most abundant and long-lived serum protein ($t_{1/2}$ in human is around 20 days) prevents not only clearance by renal filtration, but also hinders protease attack as reported in several studies.[26–28] We tested this approach and conjugated KLK5(1) and KLK7(1) to a recently developed, lipidated albumin-binding heptapeptide that binds human albumin with a K_d of 39 nM. Previous work showed that this lipidated heptapeptide prolonged the elimination half-life in rats and rabbits from minutes to approximately six hours [27]. However, a drawback of albumin-binding tags is that they often reduce the binding affinity of the peptides to their targets. For example, the lipidated heptapeptide reduced the K_is of a urokinase-type plasminogen activator and a plasma kallikrein inhibitor more than 2-fold and 100-fold, respectively.[27] We conjugated the heptapeptide albumin tag to either the N- or C-termini of the KLK5- and KLK7-inhibiting peptides KLK5(1) and KLK7(1) using a solid phase synthesis strategy (Figure 4a and Figure S6). A fluorescein moiety was included with the albumin tag in the conjugates (Figure 4b) in order to increase albumin binding and to allow for the use of fluorescence polarization to measure conjugate and albumin binding.

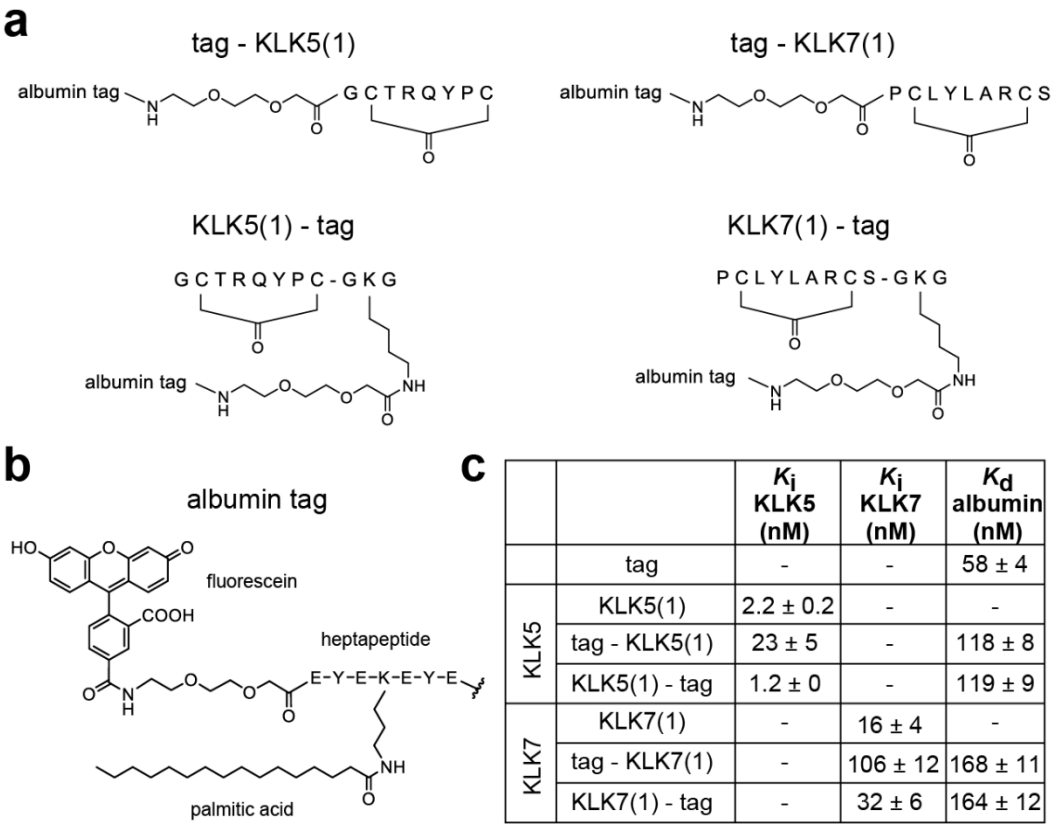

		K_i KLK5 (nM)	K_i KLK7 (nM)	K_d albumin (nM)
	tag	-	-	58 ± 4
KLK5	KLK5(1)	2.2 ± 0.2	-	-
KLK5	tag - KLK5(1)	23 ± 5	-	118 ± 8
KLK5	KLK5(1) - tag	1.2 ± 0	-	119 ± 9
KLK7	KLK7(1)	-	16 ± 4	-
KLK7	tag - KLK7(1)	-	106 ± 12	168 ± 11
KLK7	KLK7(1) - tag	-	32 ± 6	164 ± 12

Figure 4. Conjugation of KLK inhibitors to an albumin ligand. (a) Schematic depiction of conjugates. For N-terminal conjugation of the albumin ligand (tag), the tag was attached through a PEG_2 linker. For C-terminal conjugation, the tag was conjugated to a lysine sidechain of the short peptide Gly-Lys-Gly that was appended to the C-terminus of the inhibitor. (b) Structure of albumin-binding tag. (c) KLK inhibition activity and albumin binding of the four conjugates, tag alone, and inhibitors alone. Inhibition of KLK5 and KLK7 was measured in the presence of human albumin (25 μM). Data represent the means of three independent measurements ± SD.

We measured the inhibitory activity of the conjugates in presence of albumin (25 μM) because association with the serum protein could potentially hinder access to the KLKs and thus reduce inhibitor potency. Conjugation of the tag to the N-terminus reduced the potency of KLK5(1) by around 10-fold (tag-KLK5(1); K_i = 23 ± 5 nM), and reduced the potency of KLK7(1) by around 7-fold (tag-KLK7(1); K_i = 106 ± 12 nM) (Figure 4c and Figure S7a). In contrast, conjugation to the C-terminus slightly improved the activity of the KLK5 inhibitor (KLK5(1)-tag; K_i of 1.2 ± 0 nM) and nearly conserved the activity of the KLK7 inhibitor (KLK7(1)-tag; K_i = 32 ± 6 nM) (Figure 4c and Figure S7a).

We subsequently measured the binding of the conjugates to human albumin, which could easily be done in a fluorescence–polarization-based assay since all conjugates contained a fluorophore. All of the conjugates bound to human albumin with sub-micromolar affinity, wherein the affinity was around two- to three-fold reduced when compared to the tag alone (Figure 4c and Figure S7b). The two C-terminally tagged conjugates that retained KLK inhibition activity bound albumin with a K_d of around 160 nM, which promised efficient association with the serum protein and thus a long circulation time *in vivo*.

Engineering KLK inhibitors that are stable in blood plasma

We next tested the stability of the inhibitors in human plasma using a degradation assay and LC-MS analysis. Incubation of KLK5(1)-tag and KLK7(1)-tag with human plasma and LC-MS analysis revealed a high stability for the KLK5 inhibitor ($t_{1/2}$ = 90 h) but relatively fast degradation for the KLK7 inhibitor ($t_{1/2}$ = 0.4 h) (Figure 5a and Figure S8). Incubating KLK5(1) and KLK7(1) lacking the albumin tag in plasma showed rapid degradation in under five minutes for both, indicating that tethering of the peptides via the tag strongly enhances their proteolytic stability (Figure 5b and Figure S8). We reasoned that the KLK5 inhibitor KLK5(1)-tag should be sufficiently stable *in vivo* but that the stability of the KLK7 inhibitor needed to be improved.

To address the stability of the KLK7 inhibitor, we first used the LC-MS analysis of the KLK7(1)-tag after incubation in human plasma to identify the degradation products. From this analysis, the major degradation product corresponded exactly to the mass of cyclic KLK7(1), suggesting that the conjugate was cleaved between amino acid Ser9 and the first glycine of the linker (Figure 5c and Figure S9a). We then synthesized the new conjugate KLK7(2)-tag in which Ser9 and thus the vulnerable peptide bond was deleted (Figure 5d). The new conjugate had a half-life of four hours in plasma and thus a 10-fold improved stability. Further LS-MS analysis of plasma-treated KLK7(2)-tag

identified a new vulnerable region near Arg7 (Figure 5d and Figure S9b). From the synthesis of peptide variants (Figure 2b) and the SAR study (Figure 3b), we knew that a mutation of Arg7 to Gln or homoarginine (hArg) largely conserved the inhibitory activity of KLK7, and we thus synthesized peptides with these amino acid substitutions, along with a mutant where Arg was replaced with citrullin (Cit) (Figure 5e). All the three variants showed improved stability in human plasma with half-lives of longer than 4 days (Figure 5e and Figure S9c). Due to its high inhibitory activity, the conjugate KLK7(5)-tag containing Arg7 mutated to hArg was chosen along with the KLK5 inhibitor KLK5(1)-tag for *in vivo* studies (Figure S9d and Figure S10).

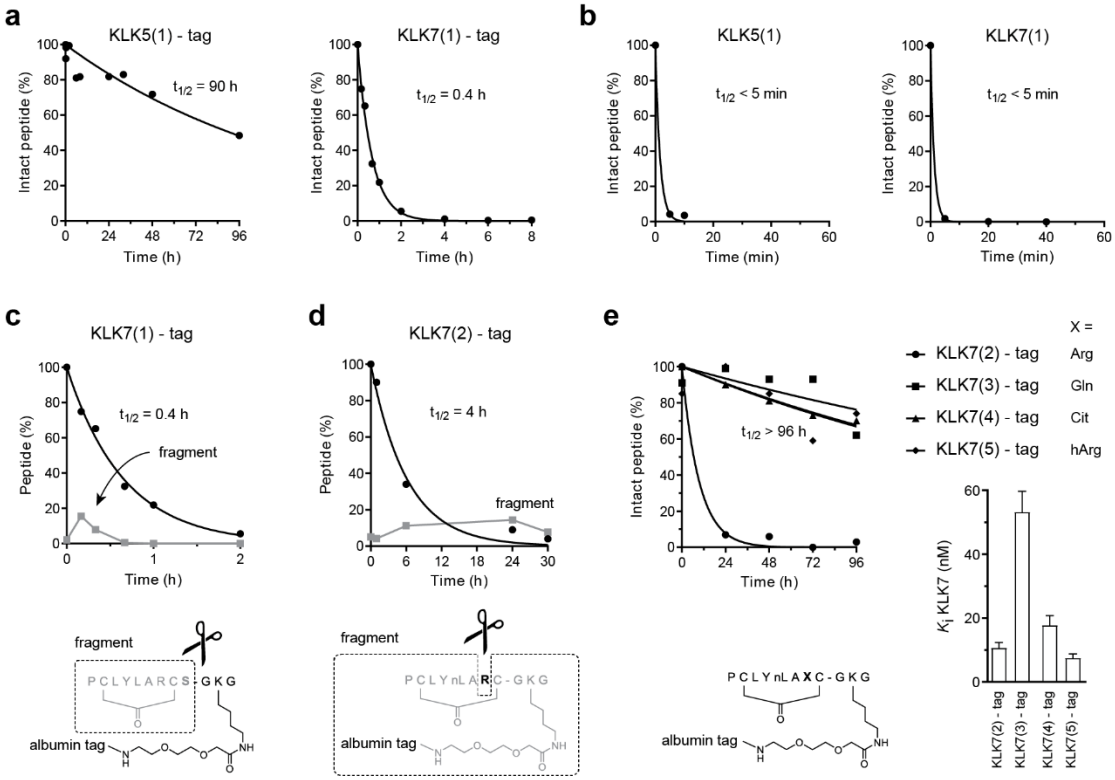

Figure 5. Proteolytic stability of conjugates in plasma and stability improvement. The stability of all conjugates was assessed by incubation in human plasma and analysis of the samples by LC-MS. (a, b) Stability of KLK5(1) and KLK7(1) (a) with or (b) without albumin-binding ligands (tag). (c) Incubation of KLK7(1)-tag in human plasma forms a degradation product (grey curve) with a mass corresponding to the cyclic peptide truncated after Ser9. (d) KLK7(2)-tag has the same structure as KLK7(1)-tag, but without Ser9 and norleucine instead of leucine in position 5 (Figure S9). A degradation product was found that corresponded with

the molecular weight of the conjugate lacking Arg7 (Figure S9). (e) Variants of KLK7(2)-tag in which Arg7 was replaced with arginine homologs. All variants showed an improved stability. Substitution to homoarginine (hArg) lead to the best KLK7 inhibition activity (KLK7(5)-tag).

Pharmacokinetics in mice

We next aimed to assess the pharmacokinetic properties of the KLK inhibitor-tag conjugates in mice. The albumin-binding tag was developed for binding to human albumin and thus has a substantially weaker affinity for the orthologous rat albumin (K_d = 220 ± 30 nM; 5.6-fold lower) and rabbit albumin (K_d = 320 ± 40 nM; 8.2-fold lower).[27] Thus, we expected a low affinity for mouse albumin as well. Indeed, fluorescence polarization binding assays with mouse albumin showed that the tag alone (tag) and the tagged KLK5 inhibitor (KLK5(1)-tag) had affinities of 4.3 ± 0.4 μM and 7 ± 1.1 μM, respectively (Figure S7c). While the binding affinity for mouse albumin was around 100-fold weaker than for human albumin, we still expected to see a prolonged effect on the inhibitor half-lives due to the high albumin concentration in blood plasma (around 0.6 mM). In parallel to testing the affinity for mouse albumin, we measured mouse KLK inhibition. The KLK5(1)-tag inhibited murine KLK5 with a K_i of 1.4 nM and KLK7(5)-tag inhibited murine KLK7 with a K_i of 4.1 nM (Figure S7d).

We applied the KLK5 inhibitor (KLK5(1)-tag) and the KLK7 inhibitor (KLK7(5)-tag) to groups of three mice each by intravenous injection (IV, 6.2 mg/kg). This dose was calculated to result in a plasma concentration of around 20 μM, assuming the mouse had 1 mL total blood plasma volume and the drug was distributed only to the plasma. We took blood samples at various time points and quantified the inhibitors by HPLC analysis and fluorescence detection, which allowed for the quantification of intact conjugates as well as degradation products carrying the fluorescein. The KLK5 and KLK7 inhibitors showed a terminal $t_{1/2}$ of 4.4 ± 0.3 hours and 6.2 ± 0.9 hours, respectively (Figure 6a and 6b, and Figure S11). These half-lives were around 10-fold longer than non-tagged bicyclic peptides specific for other targets previously assessed

in mice [26,29]. To test the effect of the injection route on the half-life, we applied the KLK5 inhibitor (KLK5(1)-tag) both intraperitoneally (IP; 6.2 mg/kg, n = 3) and subcutaneously (SC, 6.2 mg/kg, n = 3), which resulted in comparable half-lives of 5.1 ± 0.7 and 5.8 ± 0.4 hours, respectively (Figure 6a and 6b, and Figure S11).

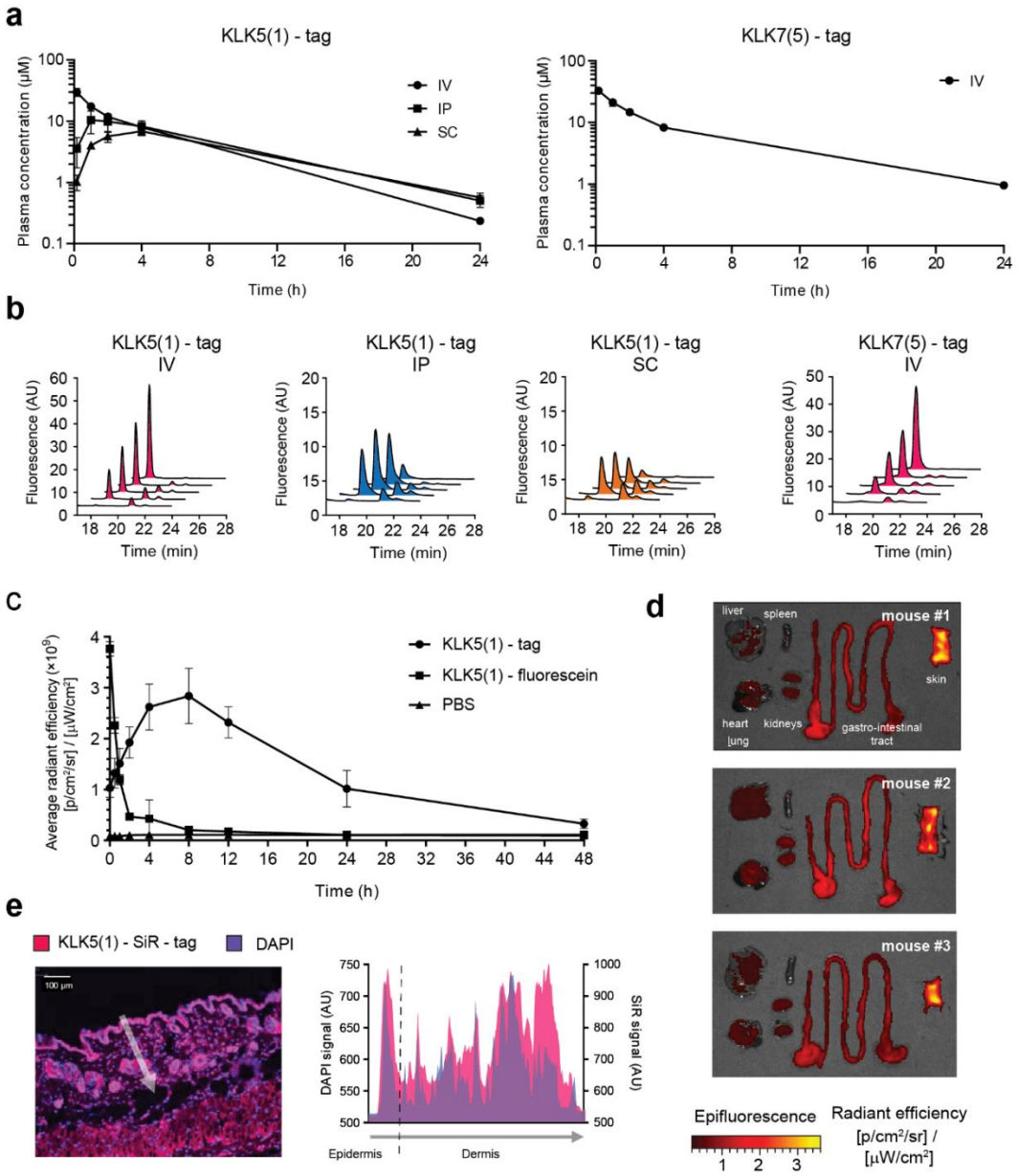

Figure 6. Pharmacokinetics and diffusion of peptide into skin. (a) Mice (n = 3 per group) were injected intravenously (IV), intraperitoneally (IP), or subcutaneously (SC) with 6.2 mg/kg of KLK5 inhibitor or KLK7 inhibitor (only IV). Blood samples were taken at different time points and analyzed by analytical HPLC equipped with a fluorescence detector. The concentration of

intact conjugate is shown. (b) HPLC chromatograms of blood samples described in (a). (c) Mice were IP injected with KLK5(1)-tag (6.2 mg/kg; 2 μmol/kg; n = 3), KLK5(1)-fluorescein (0.75 mg/kg; 2 μmol/kg; n = 3), or PBS (background control, n = 1), and the fluorescence intensity was measured at the indicated time points with a CCD camera. The average radiant efficiency in the area of the mice is shown. (d) Fluorescence imaging of skin and visceral organs 48 hrs after injection of KLK5(1)-tag (12.4 mg/kg, n = 3). (e) A mouse was injected with KLK5(1)-SiR-tag (6.4 mg/kg; 2 μmol/kg; n = 1), sacrificed after eight hours, and skin sections were analyzed by fluorescence microscopy. The SiR-tag is the same albumin-binding molecule as the tag, but with SiR instead of fluorescein as the fluorophore. SiR is excited and emits at a longer wavelength, which reduces the background fluorescence from tissue. Fluorescence is shown in red and DAPI (cell nuclei) in blue. The right graph shows the intensity profile plots of the SiR and DAPI signal along the arrows shown in the tissue section.

We also checked the stability of these inhibitors. For both inhibitors and all injection routes, the main fluorescent species observed in the RP-HPLC analysis corresponded to the intact inhibitor-tag conjugates (Figure 6b, main peak eluting at around 18 min). For both inhibitors, two small peaks eluting at around 21 min and 22 min were observed that could not be identified by mass spectrometry but indicated some *in vivo* degradation of the conjugates. These peaks were slightly larger if the inhibitor was applied IP or SC. Overall, though, these degradation peaks represented only a small amount of the total inhibitor. Thus, the limited proteolytic processing suggests that the inhibitors were primarily cleared by renal filtration and not by proteolytic degradation, and thus that the stability was sufficient for *in vivo* experiments.

KLK inhibitors are enriched in epidermis

For the inhibition of KLK5 and KLK7 in NS or other skin disorders, the inhibitors must diffuse into the epidermal layer of the skin where the two proteases are expressed and activated. We tested if the two inhibitors could diffuse into tissues and reach the epidermis after systemic application. We suspected this was feasible due to a previous study of the biodistribution of a bicyclic peptide uPA inhibitor conjugated to the albumin binding peptide SA21, wherein we observed enrichment of the conjugate in mouse skin.[29] To test the KLK inhibitors here, we first intravenously applied the KLK5(1)-tag

to mice (6.2 mg/kg, 2 μmol/kg, n = 3) and exposed the mice to light at 495 nm. We imaged the light emitted from these mice at different time points using a CCD camera. Given the low penetration of light at 495 nm (excitation) and slightly longer wavelength (emission) through tissues, we expected to only detect inhibitor that diffused into very superficial skin tissue of the mice (Figure 6c). Gratifyingly, we detected a clear signal that peaked at around 8 hours and was well above the negative control (mouse injected with PBS, n = 1). Both the steady increase of inhibitor over an 8 hour period as well as the finding that time 0 did not show the strongest signal indicated that we were indeed detecting conjugate in mouse tissue rather than in the blood stream. In a control experiment, we applied peptide KLK5(1) labeled with fluorescein, but without the albumin-binding tag (KLK5(1)-fluorescein; 3.2 mg/kg, 2 μmol/kg, n = 3). Mice treated with this control showed fluorescence emission immediately after injection and the signal faded rapidly ($t_{1/2}$ = 0.64 ± 0.04 hours), showing that the albumin binding tag was essential for the distribution of inhibitor to the tissues and skin (Figure 6c). A control experiment with albumin-binding tag alone and thus without the inhibitor showed a distribution similar to that of KLK5(1)-tag, indicating that the clearance kinetics and distribution were directed by albumin binding and not KLK5 binding (data not shown).

To assess which mouse tissue contained the fluorescence molecule, we repeated the experiment described above with a slightly higher dose (12.4 mg/kg, n = 3), sacrificed the mice after 48 hours, and dissected the skin and organs to measure fluorescence intensity directly at the surface of the organs. Exposure of the organs to light at 495 nm and measurement of the emitted light by a CCD camera revealed that the skin contained most of the conjugate, followed by the intestinal tissue (Figure 6d). In heart, lung, liver, kidney, and spleen tissue, only weak fluorescence signals were detected. While the aim of the albumin-binding tag was to prevent fast renal clearance of the KLK-inhibiting peptides, it appeared that the tag helped to enrich the inhibitors in exactly the tissues expressing KLK. This finding could be very useful in NS therapy development.

Finally, to investigate which layers of the skin the KLK5(1)-tag conjugate could reach, we microscopically analyzed skin sections. For this analysis, we synthesized the KLK5(1)-tag conjugate with the far-red fluorophore silicon rhodamine (SiR) instead of fluorescein (KLK5(1)-SiR-tag; Figure S12). SiR can be excited at around 650 nm and has an emission maximum at 674 nm, allowing fluorescence detection in a range where tissue components have lower auto fluorescence. We applied the KLK5(1)-SiR-tag to a mouse (6.4 mg/kg, 2 μmol/kg, n = 1), sacrificed the animal after 8 hours, stained sections of the skin with DAPI, and scanned the entire section with a fluorescence microscope. In a parallel control experiment to identify potential artifacts in case the fluorophore was released by proteolysis of the conjugate, we applied free SiR (0.9 mg/kg, 2 μmol/kg, n = 1) to another mouse. SiR signal was found in various regions in the skin of mice treated with KLK5(1)-SiR-tag, including the epidermis (Figure 6e and Figure S13a), but not in skin sections of mice treated with SiR (Figure S13b). These results showed that a KLK inhibitor conjugated to an albumin ligand can be efficiently delivered to the KLK targets in the skin. Given that human skin is different than that of mice, and that skin of NS patients is additionally thickened due to keratinocyte hyperproliferation, it will be important to assess if the conjugate is similarly enriched in the epidermis of NS patients. A next step in the development will be the assessment of the pharmacological activity of the inhibitors in animal models. Positive results in an animal study could lead to the development of specific treatments for NS based on the use of our synthetic KLK inhibitors.

CONCLUSIONS

To advance NS therapy research, we screened the largest reported cyclic peptide phage display library to our knowledge, comprising more than 100 billion different cyclic peptides. Through this screen, we identified potent KLK5 and KLK7 inhibitors with K_is in the single-digit nanomolar range. The inhibitors we identified are slightly weaker than the best KLK inhibitors reported, but improve upon existing inhibitors in that they are substantially smaller and easier to synthesize and conjugate. Stability-improved variants of our phage-selected inhibitors are stable in blood for hours, and due to their conjugation to a peptidic albumin tag, our variants have a prolonged circulation time *in vivo* (mice) compared to previously reported inhibitors. It is likely that these inhibitors have an even longer half-life in humans due to the substantially higher affinity of the inhibitor conjugates for human vs. mouse albumin. Biodistribution studies in mice with the albumin–tag-conjugated inhibitor of KLK5 confirmed the usefulness of our strategy by showing that the molecule diffused into tissues and was even enriched in the epidermis of mouse skin, where the KLKs are expressed, and their activity needs to be controlled. With their good binding properties, high stability, and distribution to skin, the peptide-based inhibitors to KLK5 and KLK7 presented herein are promising candidates for developing an NS therapy.

EXPERIMENTAL SECTION

KLK5 cloning, expression, activation and purification

DNA coding for a secretion sequence (BM40 secretory signal peptide), the human KLK5 pro-domain, Asn30-Ser293 of human KLK5 (UniProtKB Q9Y337) and a C-terminal poly-histidine tag was cloned into pEXPR-IBA42 for secreted expression in mammalian cells using the *Nhe*I and *Hind*III restriction sites. The following synthetic, codon-optimized DNA was ordered from Eurofins and was delivered in the pEX-A2 vector:

5'-
GCTAGCAATAATGATGTTAGCTGTGACCATCCATCTAATACTGTACCGTCAGGCTC
AAATCAAGACTTGGGGGCAGGAGCAGGCGAAGACGCAAGAAGCGACGACAGC
TCTTCACGA**ATTATAAACGGCTCCGATTGCGACATGCACACGCAACCCTGGCA**
AGCCGCTTTGCTTCTGAGGCCCAATCAACTTTACTGTGGAGCAGTTCTTGTCCA
CCCTCAGTGGCTGCTGACAGCCGCTCACTGCAGAAAGAAAGTCTTTAGAGTG
CGCTTGGGGCACTATTCTCTTTCACCCGTGTACGAATCTGGTCAGCAGATGTTT
CAGGGCGTAAAGTCCATACCGCACCCGGGTTATTCCCATCCCGGCCACAGTAA
CGATTTGATGTTGATAAAACTTAACAGACGGATAAGGCCAACTAAGGACGTGA
GACCTATTAACGTATCTTCTCATTGCCCGAGTGCTGGTACTAAGTGCCTGGTAA
GTGGCTGGGGCACAACAAAGTCACCTCAGGTTCACTTCCCCAAAGTACTGCA
GTGCCTGAATATCTCCGTGCTTTCACAAAAAAGATGTGAGGACGCATATCCTAG
ACAGATCGACGACACGATGTTCTGCGCGGGTGATAAAGCGGGTCGGGACTCA
TGTCAAGGGGATTCAGGAGGGCCTGTTGTTTGCAATGGATCTTTGCAAGGACT
CGTGAGCTGGGGCGATTACCCTTGCGCGAGACCCAATAGACCTGGAGTTTATA
CTAATCTCTGTAAATTCACGAAGTGGATTCAGGAAACAATCCAAGCTAATTCTG
GCAGTGGCTCCCACCATCATCACCACCACTAAGCTT-3'

(underlined: *Nhe*I and *Hind*III restriction sites, in bold: mature protease).

Insertion of the DNA into pEXPR-IBA42 yielded vector pPG001 that codes for the following protein sequence:

*MRAWIFFLLCLAGRALA*ASNNDVSCDHPSNTVPSGSNQDLGAGAGEDARSDDSSS
R**IINGSDCDMHTQPWQAALLLRPNQLYCGAVLVHPQWLLTAAHCRKKVFRVRLGH**
YSLSPVYESGQQMFQGVKSIPHPGYSHPGHSNDLMLIKLNRRIRPTKDVRPINVSS
HCPSAGTKCLVSGWGTTKSPQVHFPKVLQCLNISVLSQKRCEDAYPRQIDDTMFC
AGDKAGRDSCQGDSGGPVVCNGSLQGLVSWGDYPCARPNRPGVYTNLCKFTK
WIQETIQANSGSGSHHHHHH

(in italics: BM40 secretory signal peptide, in bold: mature protease).

The protein was expressed at the EPFL Protein Expression Core Facility by transient transfection of CHO cells cultured in solution as described before[30] but in a smaller culture volume of 100 mL. An amount of 0.3 mg of the DNA plasmid (in milliQ water; 1 mg/mL) was transfected into the cells using polyethyleneimine (PEI; linear 25 kDa, 1 mg/mL in milliQ water, pH 7.0) and the culture incubated at 31 °C, 5% CO_2 and 120 rpm. After one hour of transfection, 2 mL DMSO were added to the culture and the culture incubated for one week.

Cells were removed by centrifugation and the pH of the supernatant adjusted to 8.0 by addition of NaOH. The hKLK5 was purified from the supernatant by nickel-charged immobilized metal affinity chromatography (IMAC) using a HisTrap™ Excel column (GE Healthcare) using a binding buffer (15 mM imidazole, 200 mM NaCl, 10 mM EPPS, pH 8.0) and an elution buffer (500 mM imidazole, 200 mM NaCl, 10 mM EPPS, pH 8.0). After elution, the buffer was exchanged to 200 mM NaCl, 10 mM EPPS, pH 8.0 and the protein concentrated to around 1 mg/mL using a centrifugal contractor (MacroSep Advance 10 K MWCO, Pall Corporation). Around 5 mg purified hKLK5 were obtained from a 100 mL culture. Activity measurement and SDS-PAGE analysis showed that a substantial fraction of the zymogen was activated during expression or purification.

KLK7 cloning, expression, activation and purification (first strategy)

DNA coding a secretion sequence (BM40 secretory signal peptide), a ubiquitin sequence (reported to improve expression yields,[31] an enterokinase cleavage site (VDDDDK), mature human KLK7 (UniProtKB P49862, Ile30-Arg253), and a C-terminal poly-histidine tag was cloned into pEXPR-IBA42 using *Nhe*I and *Hind*III restriction sites. The following codon-optimized DNA sequence was ordered from Eurofins and was delivered in the pEX-A2 vector:

5'-
GCTAGCATGCAAATTTTCGTCAAGACACTCACAGGGAAAACGATTACCTTGGAGG
TGGAGCCGTCAGACACTATTGAGAATGTGAAAGGCAAAATTCAAGAGAAGGAAG
GTATCCCACCAGATCAACAAAGGCTCATTTTTGCAGGCAAGCAATTGGAGGACG
GGCGGACGTTGAGCGACTACAACATACAGAAAGAAAGCACTTTGCATCTGGTCC
TTCGGTTGAGAGGCGGGGCAGACCCAGTAGACGACGATGATAAA**ATTATTGACG**
GAGCCCCGTGCGCCCGCGGCTCACATCCATGGCAGGTAGCACTCTTGAGTGG
TAATCAGCTGCACTGTGGTGGCGTATTGGTCAATGAAAGATGGGTACTGACCG
CCGCGCATTGCAAAATGAATGAGTACACTGTTCATCTCGGTTCAGATACCTTGG
GCGACAGAAGAGCCCAGAGGATCAAAGCGTCTAAGTCCTTCCGCCACCCTGG
TTATTCTACGCAAACTCATGTAAACGACCTCATGCTCGTGAAGCTGAACAGTCA
GGCCCGATTGTCAAGTATGGTTAAAAAAGTTAGGCTCCCGAGCCGCTGTGAAC
CACCAGGCACTACATGCACGGTAAGCGGGTGGGGTACAACAACGTCTCCAGA
CGTCACCTTCCCTAGCGACCTGATGTGCGTGGATGTCAAGCTGATCTCACCTC
AAGATTGCACGAAAGTATATAAAGACCTCTTGGAGAACTCCATGCTGTGTGCTG
GTATTCCCGATAGCAAAAAGAATGCGTGTAATGGCGATTCAGGGGGTCCCCTT
GTGTGCCGGGGCACCCTCCAAGGGCTCGTTAGCTGGGGCACCTTTCCTTGCG
GCCAGCCTAACGATCCAGGTGTGTACACCCAGGTATGTAAATTCACAAAATGG
ATCAATGATACCATGAAAAAGCACAGGGGCAGTGGCTCCCACCATCATCACCA
CCACTAAGCTT-3'

(underlined: *Nhe*I and *Hind*III restriction sites, in bold: mature protease).

Insertion of the DNA into pEXPR-IBA42 yielded the vector pPG002 that codes for the following protein sequence:

*MRAWIFFLLCLAGRALA*ASMQIFVKTLTGKTITLEVEPSDTIENVKGKIQEKEGIPPDQ
QRLIFAGKQLEDGRTLSDYNIQKESTLHLVLRLRGGADPVDDDDK**IIDGAPCARGSH**
PWQVALLSGNQLHCGGVLVNERWVLTAAHCKMNEYTVHLGSDTLGDRRAQRIKA
SKSFRHPGYSTQTHVNDLMLVKLNSQARLSSMVKKVRLPSRCEPPGTTCTVSGW
GTTTSPDVTFPSDLMCVDVKLISPQDCTKVYKDLLENSMLCAGIPDSKKNACNGD
SGGPLVCRGTLQGLVSWGTFPCGQPNDPGVYTQVCKFTKWINDTMKKHRGSGS
HHHHHH

(in italics: BM40 secretory signal peptide, underlined: enterokinase cleavage site, in bold: mature protease).

The protein was expressed by transient transfection of CHO cells cultured in solution and purified by IMAC as described above. Around 1.5 mg of protein were obtained from a 100 mL culture. The human KLK7 preceded by an ubiquitin sequence and an

enterokinase cleavage site was activated by treatment with 0.04 U enterokinase (Sigma-Aldrich) per μg hKLK7 at 37 °C overnight in 20 mM Tris-HCl, 50 mM NaCl, 2 mM $CaCl_2$, pH 8.0 and purified again by IMAC. The buffer was exchanged to 200 mM NaCl, 10 mM EPPS, pH 8.0 and the protein concentrated to around 1 mg/mL using a centrifugal contractor (MacroSep Advance 10 K MWCO, Pall Corporation). SDS-PAGE analysis showed that the KLK7 was activated quantitatively. Around 0.2 mg mature hKLK7 was obtained from a 100 mL culture. The KLK7 protein was used for phage selections.

KLK7 cloning, expression, activation and purification (second strategy)

With the goal of producing human KLK7 that was readily auto-activated after expression or purification, we cloned a construct with an artificial pro-domain (KLK5 pro-domain) wherein the last two amino acids of KLK5 pro-domain (Ser-Arg) were replaced with the substrate-recognition sequence of KLK7 (Tyr-Leu). Towards this end, the DNA coding for the pro-domain of KLK5 was amplified from pEX-A2-hKLK5 using the primer pair oPG001F and oPG002R and the DNA coding for mature human KLK7 (UniProtKB P49862, Ile30-Arg253) was amplified from pEX-A2-hKLK7 using the primer pair oPG003F and oPG004R. The two PCR products were fused in another PCR using the primer pair oPG001F oPG004R and the two pervious PCR products as templates. The Fusion-PCR product was cloned into pEXPR-IBA42 using *Nhe*I and *Hind*III restriction sites.

Primer oPG001F: gatcGCTAGCAATAATGATGTTAGCTGTGACCATC

Primer oPG002R: ctccgtcaataatgtacagAGAGCTGTCGTCGCTTCTTGC

Primer oPG003F: cgacgacagctctctgtacATTATTGACGGAGCCCCGTGC

Primer oPG004R: atgcAAGCTTAGTGGTGGTGATGATGGTGGGAGC

(uppercase: binding region, lowercase: overhangs, underlined: *Nhe*I and *Hind*III restriction sites).

Insertion of the DNA into pEXPR-IBA42 yielded a DNA that encodes for the following protein sequence:

*MRAWIFFLLCLAGRALA*ASNNDVSCDHPSNTVPSGSNQDLGAGAGEDARSDDSSL
Y**IIDGAPCARGSHPWQVALLSGNQLHCGGVLVNERWVLTAAHCKMNEYTVHLGS
DTLGDRRAQRIKASKSFRHPGYSTQTHVNDLMLVKLNSQARLSSMVKKVRLPSR
CEPPGTTCTVSGWGTTTSPDVTFPSDLMCVDVKLISPQDCTKVYKDLLENSMLCA
GIPDSKKNACNGDSGGPLVCRGTLQGLVSWGTFPCGQPNDPGVYTQVCKFTKWI
NDTMKKHR**GSGSHHHHHH

(in italics: BM40 secretory signal peptide, underlined: KLK7 cleavage site, in bold: mature protease).

The protein was expressed by transient transfection of CHO cells cultured in solution and purified by IMAC as described above. Around 1.5 mg mature human KLK7 were obtained from a 100 mL culture. The buffer was exchanged to 200 mM NaCl, 10 mM EPPS, pH 8.0 and the concentration adjusted to around 1 mg/mL using a centrifugal contractor (MacroSep Advance 10 K MWCO, Pall Corporation). SDS-PAGE analysis showed that the KLK7 was activated quantitatively.

KLK biotinylation and immobilization

Recombinantly expressed hKLK5 and hKLK7 (hKLK7 produced following the first strategy described above) were immobilized on magnetic beads by random biotinylation of amino groups and addition to streptavidin or NeutrAvidin magnetic beads. Biotinylation was conducted by incubating the proteins at a concentration of 10 μM in an amine-free buffer (200 mM NaCl, 10 mM EPPS, pH 8.0) with 20 equiv. of EZ-Link™ Sulfo-NHS-LC-Biotin (ThermoFisher Scientific). Sulfo-NHS-LC-Biotin was freshly dissolved at 10 mg/mL in DMSO, added to the proteins, and incubated for 1 hr. Excess biotinylation reagent was removed by size exclusion chromatography using a disposable PD-10 desalting column (GE Healthcare) and PBS buffer (PBS, pH 7.4,

- $CaCl_2$, - $MgCl_2$, 10010023 Gibco, Thermo Fisher Scientific [Waltham, MA, USA]). The

percentage of biotinylated KLK was assessed by capturing 1 μg of biotinylated protein on 25 μL streptavidin magnetic beads (Dynabeads™ M-280 Streptavidin from ThermoFisher Scientific) and subsequent analysis of immobilized protein by SDS-PAGE as previously described [32]. In the three rounds of phage selection either 50 μL streptavidin magnetic beads (first and third round) or 20 μL NeutrAvidin magnetic beads (second round) were used. NeutrAvidin beads were prepared by coupling 6 mg NeutrAvidin (ThermoFisher Scientific) to 10 mL tosyl-activated magnetic beads (Dynabeads™ M-280 Tosylactivated from ThermoFisher Scientific) according to the manufacturer's protocol. The 50 μL streptavidin magnetic beads or 20 μL NeutrAvidin magnetic beads were washed twice with 1 mL washing buffer (10 mM Tris-HCl, 150 mM NaCl, 10 mM $MgCl_2$, 1 mM $CaCl_2$, pH 7.4) and resuspended in 50 μL washing buffer. In the first, second and third round of panning, 10 μg, 5 μg and 2.5 μg hKLK5 or hKLK7 were immobilized on the magnetic beads, respectively, by incubation for 10 min on a rotating wheel. The beads were washed three times with 1 mL washing buffer and blocked by incubation in 0.5 mL washing buffer containing 1 % (w/v) BSA and 0.1 % (v/v) Tween-20 for 30 min on a rotating wheel.

Cyclic peptide phage display library production

Phage displaying peptides of the format $XCX_mCX_nCX_oCX$ (m + n + o = 12)[22] were produced as follows. For each target and cyclization linker, one liter 2×YT medium complemented with 100 μg/mL ampicillin and 100 mM glucose was inoculated with glycerol stock of the phage library to reach an OD_{600} of 0.1 and grown at 37 °C at 200 rpm. At OD_{600} = 0.5 the culture was infected with an excess of hyperphage (Progen) and incubated for 15 min at 37 °C without shaking. The number of cells successfully infected with hyperphage was 2.5×10^{10}. After infection, the culture was incubated another 45 min at 37 °C and 250 rpm to allow expression of the gene providing kanamycin resistance. To remove the glucose, the bacteria were pelleted by centrifugation for 10 min at 2,000 × g and 4 °C and resuspended in one liter of 2×YT with 100 μg/mL ampicillin and 50 μg/mL kanamycin. Phage were produced overnight

at 30 °C and 200 rpm. For the second and third round of phage selection, phage were produced in 100 mL cultures.

Phage from one liter cultures (100 mL cultures in round 2 and 3) were purified by precipitation with ¼ volume of 20% (w/v) PEG6000/ 2.5 M NaCl as previously described, resuspended in 20 mL reaction buffer (20 mM NH_4HCO_3, 5 mM EDTA, pH 8, degassed; 10 mL in round 2 and 3), and reduced by incubation with tris(2-carboxyethyl)phosphine (TCEP, 1 mM final concentration) for 30 min at RT. Phage were precipitated with ¼ volume of PEG6000/NaCl and resuspended in 9 mL (also 9 mL in round 2 and 3) reaction buffer, and the peptides cyclized by addition of 1 mL (also 1 mL in round 2 and 3) of 0.4 mM BBMP or DBA in 10% acetonitrile, 90% H_2O (freshly prepared) to reach final concentrations of 40 μM. The reactions were incubated in a water bath for 1 hr at 30 °C, the phage purified by PEG-precipitation and resuspended in 5 mL washing buffer (10 mM Tris-HCl, 150 mM NaCl, 10 mM $MgCl_2$, 1 mM $CaCl_2$, pH 7.4) containing 1 % (w/v) BSA and 0.1 % (v/v) Tween-20.

Phage display panning

Magnetic beads with immobilized hKLK5 or hKLK7 were added to 5 mL phage library and incubated for 30 min on a rotating wheel (5 rpm) at RT. The beads were subsequently washed three time with 1 mL washing buffer containing 0.1% (v/v) Tween-20 and six times with 1 mL washing buffer. The tubes were changed after every third wash to avoid carrying along phage sticking to the tubes. Phage were eluted by resuspension of the beads with 100 μL glycine buffer (50 mM, pH 2.2) and incubation for 5 min. The beads were separated in a magnetic rack and the supernatant was transferred into a new tube containing 100 μL 1 M Tris-HCl, pH 8.0 for neutralization. Eluted phage were added to 10 mL exponentially growing TG1 *E. coli* cells (OD_{600} = 0.5) and incubated for 30 min at 37 °C without shaking. The infected cells were centrifuged for 10 min, 3,000 × g at 4 °C and resuspended in 1 mL 2×YT medium by

pipetting. The resuspended cells were plated on 15 cm 2×YT plates containing 100 μg/mL ampicillin and incubated at 37 °C overnight. The next day, cells were harvested with 4 mL 2×YT medium and glycerol was added to a final concentration of 10 % (v/v). Aliquots of 500 μL were frozen in liquid nitrogen, stored at -80 °C and used for subsequent selection rounds and sequencing.

Phage DNA sequencing

A volume of 15 μL *E. coli* glycerol stock was suspended in 1.5 mL 2×YT and the OD_{600} was measured. The cells were diluted to 500 cells/mL by serial dilution and 1 mL was plated on a 15 cm 2×YT plate containing 100 μg/mL ampicillin. After incubation overnight at 37 °C, 96 clones were picked and 100 μL 2×YT with 100 μg/mL ampicillin in a 96 well plate. The cells were incubated for 2-3 hrs at 37 °C under shaking conditions and 2 μL of the culture was used as template for a PCR reaction in a volume of 50 μL containing Taq polymerase buffer, 200 μM dNTP, 200 nM of each primer, and 1 unit Taq polymerase (25 cycles, 30 s 95°C, 30 s 55°C, 30 s 72°C). The forward primer pSEX81_seq0 with the sequence 5'- GTGTGGAATTGTGAGCGGATAAC-3' and the reverse primer B-insert with the sequence 5'-CACCACCAGAGCCGCCGCCAGCATTGACAGGAGGTTGAG-3' were used. The amplified inserts were sent for Sanger Sequencing (Macrogen). For the sequencing reaction, the primer pSEX81_seq0 was used.

Peptide synthesis

Peptides were synthesized on solid phase on rink amide AM resin (loading 0.3 mmol/g) at a 50 μmol scale using Fmoc chemistry on an Intavis MultiPep RSi peptide synthesizer. Reagents were prepared at the following concentrations in DMF: 0.5 M Fmoc amino acids, HATU (0.5 M), and 4 M NMM (4-methylmorpholine) base. NMP (1-methyl-2-pyrrolidinone) was prepared undiluted. HATU (4 equiv., 400 μL total), base NMM (8 equiv., 100 μL), NMP (5 μL) and Fmoc amino acids (4.2 equiv., 420 μL) were

transferred in this order to a pre-mixing tube and the mixture was transferred to the resin. The amino acids were coupled twice for 30 min and shaking at 500 rpm. After coupling of each amino acid, a capping step was carried out using a solution of 5% (v/v) acetic anhydride and 6% (v/v) 2,6-lutidine in DMF (5 min, 800 μL). After the capping, the resin was washed seven times with 4 mL DMF.

Conjugation of fluorescein and palmitic acid

For conjugation of the albumin-binding tag to the peptides' C-termini and conjugation of palmitic acid to a lysine side chains, lysine with a Dde (4,4-dimethyl-2,6-dioxocyclohex-1-ylidene)ethyl) protecting group was introduced into the peptides using Fmoc-Lys(Dde)-OH (Iris Biotech GmbH). The Dde-protected side chain was removed by incubating the resin with 2% (v/v) hydrazine hydrate in DMF (4 mL, 3 min, 700 rpm) for three times. As 2% hydrazine hydrate eliminates Fmoc groups, the N-terminal amino acid of the peptides was chosen to be Boc-protected. 5(6)-carboxyfluorescein (ThermoFisher Scientific) or palmitic acid (TCI) were conjugated to the N-terminus or the side chain of lysine by adding the following reagents in the indicated order: 3.5 equiv. fluorescein or palmitic acid (0.05 M in DMF, 3500 μL; 0.05 M final concentration), 3 equiv. HATU (0.5 M in DMF, 300 μL; 0.04 M final concentration), 6 equiv. NMM (4 M in DMF, 75 μL; 0.05 M final concentration) and NMP (5 μL). The reactions were performed twice for 90 min at 700 rpm.

Peptide cleavage

Before cleavage, the resin was washed twice with DCM. Peptides were cleaved from the resin under reducing conditions by addition of 5 mL cleavage mixture (90% (v/v) TFA, 2.5% (v/v) 1,2-ethanedithiol, 2.5% (w/v) phenol, 2.5% (v/v) thioanisole, 2.5% (v/v) H_2O) for 2 hrs under shaking conditions. The cleavage mixture was separated from the resin by vacuum filtration. For fatty acid-coupled peptides, a second cleavage round was performed with another 5 mL cleavage mixture for 2 hrs under shaking conditions

while the first 5 mL were kept at RT. The second cleavage solution was separated by filtration and pooled with the first one. Peptide was precipitated by addition of 40 mL ice-cold diethyl ether and incubation at -20 °C for 30 min. Precipitated peptide was pelleted by centrifugation (10 min, 4,300 × g, 4 °C). The supernatant was removed and the pellet was washed sequentially with 30 mL and 20 mL diethyl ether.

Peptide cyclization

Around 50 μmol of crude peptide was dissolved in 9 mL 40% acetonitrile and 60% buffer (60 mM NH_4HCO_3, 5 mM EDTA, pH 8.0, degassed) and 1.5 equiv. of BBMP or DBA dissolved in 1 mL acetonitrile was added. The final concentrations in the reaction mixture were around 5 mM peptide, 7.5 mM BBMP or DBA, 50% aqueous buffer, and 50% acetonitrile. For peptides not conjugated to a fatty acid, 75% aqueous buffer and 25% acetonitrile was used. The reactions were incubated for 1 hr at 30°C, and stopped by addition of 200 μL acetic acid. The solution was lyophilized and peptides purified by RP-HPLC.

Peptide purification

Crude peptide of around 100 mg were purified by semi-preparative and preparative RP-HPLC, respectively. Preparative RP-HPLC purification was performed on a PrepLC 4000-Waters system using a C18 column (Vydac C18 TP1022, 250×22 mm, 10 μm, 300 Å), a linear gradient of solvent B (99.9% acetonitrile, 0.1% TFA) over solvent A (99.9% H_2O, 0.1% TFA) at a flow of 20 mL/min for 40 min. Absorbance was recorded at 220 nm. Fractions containing product were identified by ESI-MS (Shimadzu LCMS 2020), pooled and lyophilized.

All compounds are >95% pure by HPLC analysis. Three out of the more than 100 cyclic peptides are mixtures of two peptides. We provide the HPLC traces and MS spectra for all the more than 100 cyclic peptides produced for this study in the Supporting

Information.

Conjugation of silicon rhodamine to peptides

Silicon rhodamine was coupled to peptides via an amino group in solution. One μmol of pure peptide was dissolved in 475 μL DMSO and 25 μL of DIPEA added. To the peptide, 1.2 equiv. N-hydroxysuccinimide (NHS) ester of 6-carboxy silicon rhodamine (SiR) in 0.5 mL DMSO was added. The final concentrations in the reaction mixture were 1 mM peptide, 1.2 mM SiR-NHS ester, 2.5% (v/v) DIPEA. The reaction mixture was incubated for 1 hr at RT and purified by RP-HPLC as described above.

Synthesis of chromogenic KLK7 substrate

The synthesis of the KLK7 substrate KHLY-pNA[11] was performed according to a procedure described by Fairlie and co-workers[33] and purified by semi-preparative RP-HPLC.

Measurement of protease inhibition

The K_i values of the peptides were determined by measuring residual protease activity at varying peptide concentrations. For the KLK5 inhibitors, 0.6 μM peptide stock solutions were prepared in activity assay buffer containing freshly added BSA (200 mM NaCl, 10 mM Tris-Cl, pH 8.0, 0.01 % (v/v) Triton-X100, 0.1 % BSA (w/v, 1 mg/mL)). Ten 2-fold serial dilutions were prepared using the same buffer. The fluorogenic substrate Boc-VPR-AMC (Bachem) was diluted to 300 μM and hKLK5 to 3 nM in activity assay buffer. 50 μL peptide, 50 μL hKLK5 and 50 μL substrate were pipetted into a transparent, 96 well flat-bottom plate resulting in final concentrations of 200 nM to 0.2 nM peptide, 1 nM enzyme and 100 μM substrate in the assay. The residual proteolytic activity was determined at 25 °C by measuring the rate of AMC formation over 30 min, using a fluorescence plate reader (Tecan Infinite M200 Pro) and excitation

and emission wavelengths of 368 and 467 nm, respectively.

For the KLK7 inhibitors, 12 μM peptide stock solutions were prepared in activity assay buffer and ten 2-fold serial dilutions were prepared using the same buffer. The chromogenic substrate KHLY-pNA (100 mM stock in DMSO) was diluted to 1200 μM and hKLK7 to 30 nM in activity assay buffer. 50 μL peptide, 50 μL hKLK7 and 50 μL substrate were pipetted into a transparent, 96 well flat-bottom plate resulting in final concentrations of 4 μM to 4 nM peptide, 10 nM enzyme and 400 μM substrate in the assay. The residual proteolytic activity was determined at 25 °C by measuring the rate of pNA formation over 30 min, using an absorption plate reader (Tecan Infinite M200 Pro) and measurement of absorption at 405 nm.

The IC_{50} values were determined by fitting sigmoidal curves to the data using the following four-parameter logistic equation:

$$Y = \frac{100}{1 + 10^{(\mathrm{Log}IC_{50} - X)p}}$$

Wherein Y is the residual activity (%) of protease, X is the logarithm of peptide concentration, IC_{50} is the concentration of inhibitor that produces 50% inhibition, and p is the Hill coefficient. The K_i values were calculated based on the IC_{50}s using the Cheng-Prusoff equation:

$$K_i = \frac{IC_{50}}{1 + \frac{[S]_0}{K_m}}$$

Wherein $[S]_0$ is the initial concentration of substrate, and K_m is the Michaelis-Menten constant for the enzyme and substrate pair. The K_m value for hKLK5 and Boc-VPR-AMC was determined to be 216 μM. The K_m value of hKLK7 and KHLY-pNA was 107 μM.

Inhibition of mouse KLK5 (mKLK5; Bio-Techne) was measured using the same conditions as for hKLK5.

Specificity profiling

The target specificity was assessed by incubating a panel of human proteases individually with the inhibitors in 96-well plates and measuring residual protease activity using coumarin-based fluorogenic peptide substrates and a fluorescence plate reader (Tecan Infinite M200 Pro). The following concentrations of enzyme were used: 0.25 nM plasma kallikrein, 2 nM factor XIIa, 2 nM thrombin, 1.5 nM uPA, 7.5 nM tPA, 2.5 nM plasmin, 0.1 nM trypsin. The following fluorogenic substrates were used at 50 μM final concentration: Z-Phe-Arg-AMC for plasma kallikrein, Z-Gly-Gly-Arg-AMC for factor XIIa, thrombin, uPA, tPA and trypsin, H-D-Val-Leu-Lys-AMC for plasmin.

Measurement of albumin binding

Two-fold serial dilutions of human serum (Sigma-Aldrich, HSA concentration was assumed to be 600 μM) or MSA (Sigma-Aldrich, 600 μM in PBS) were prepared in FP assay buffer (10 mM Na_2HPO_4, 1.8 mM KH_2PO_4, pH 7.4, 137 mM NaCl, 2.7 mM KCl, 0.01% (v/v) Tween-20). The serial dilutions (45 μL) and fluorescent peptide (15 μL, 100 nM in FP assay buffer) were pipetted into a black, 96 well half-area microtiter plate. The final protein concentration in the plate ranged from around 30 μM to 30 nM for HSA in human serum and from around 350 μM to 170 nM for MSA, whereas the final fluorescent peptide concentration was 25 nM in all wells. Fluorescence anisotropy was measured using a plate reader (Tecan Infinite M200 Pro) with an excitation filter at 485 nm and an emission filter at 535 nm. The K_d values were determined by nonlinear regression analysis of anisotropy versus protein concentration using the following equation:

$$A = A_f + (A_b - A_f) * \left[\frac{([L]_T + K_d + [P]_T) - \sqrt{([L]_T + K_d + [P]_T)^2 - 4[L]_T * [P]_T}}{2[L]_T} \right]$$

A_f and A_b = fluorescence anisotropy for free and the fully bound fluorescent ligand, $[L]_T$ and $[P]_T$ = total fluorescent ligand and protein concentration, K_d = dissociation constant

Determination of plasma stability

Peptides were added to a final concentration of 80 μM in 300 μL human plasma (citrated, Innovative Research) and incubated at 37 °C. Samples of 15 μL were taken at various time points and 5 μL guanidinium hydrochloride solution (7 M, pH 2.0, adjusted with HCl) was added to each sample taken, to denature plasma proteins. Samples were vortexed, incubated for 10 min at RT and stored at -20 °C until the end of the experiments, when the samples were analyzed. To each 20 μL sample, 200 μL ice-cold EtOH / TFA (99.9 : 0.1) was added and the samples were incubated for 30 min at 4 °C to precipitate plasma proteins. Precipitated proteins were pelleted by centrifugation (15,000 × g, 4 ˚C, 20 min) and the supernatants were transferred into fresh tubes. EtOH was evaporated at 50 °C using a vacuum concentrator. The dry pellets were dissolved in 40 μL H_2O / formic acid (99.9 : 0.1) and 5 μL samples were analyzed by LC-MS (Shimadzu LCMS 2020) using a C18 column (Phenomenex Kinetex® column, 50 × 2.1 mm, 2.6 µm, 100 Å) and a linear gradient of solvent B (94.95% acetonitrile, 5% H_2O, 0.05% HCOOH) in solvent A (94.95% H_2O, 5% acetonitrile, 0.05% HCOOH) from 0 – 30% (mono- and bicyclic inhibitors) or 10 – 65% (inhibitor-tag conjugates) in 4.5 min at a flow rate of 1 mL/min. ESI-MS detection was done in positive mode. The quantity of intact peptides or degradation products was estimated based on the total ion current (TIC) chromatograms. The peak intensities of intact peptide or degradation products were compared to the intensity of intact peptide that was not incubated with plasma. The half-lives of peptides were determined by fitting the data to a one-phase decay model using GraphPad Prism software.

Determination of pharmacokinetics in mice

All experiments in mice were conducted in accordance with the terms of the Swiss

animal protection law and were approved by the animal experimentation committee of the cantonal veterinary service (Canton of Vaud, Switzerland). For all experiments, male C57BL/6J mice (Charles River) with a weight of around 20 g were used. Mice were IV, IP or SC injected with 6.2 mg/kg KLK5 inhibitor or KLK7 inhibitor dissolved at a concentration of 400 µM injection buffer (184 mM propylene glycol, 8 mM Na_2HPO_4 2 H_2O, pH 7.4; containing 0.4 % DMSO for the KLK5 inhibitor and 1.4 % DMSO for KLK7 inhibitor; sterile filtered). The injection volumes were around 100 µL for a 20 g mouse. Blood samples of 20 µL were taken at different time points into EDTA coated tubes (Microvette® 100 µL, EDTA from Sarstedt). The samples were centrifuged (5 min, 4 °C, 2000 × g) and plasma was separated and stored at -80 °C. To plasma samples of 5 µL, 2 µL a fluorescein-conjugated albumin binding peptide (0.1 mM in PBS; 200 pmol) was added as standard. 5 µL guanidinium hydrochloride solution (7 M, pH 2.0, adjusted with HCl, filtered) was added and the samples were vortexed and incubated for 10 min at RT. Plasma proteins were precipitated with EtOH / TFA and removed by centrifugation as described above and EtOH was evaporated. Dried pellets were dissolved in 113 µL H_2O / TFA (99.9 : 0.1) and 95 µL were analyzed on a C18 column (Agilent Zorbax 300SB-C18, 4.6 mm×250 mm, 5 µm) using an analytical RP-HPLC (Agilent 1260 HPLC system) equipped with a fluorescence detector (Shimadzu RF-10AXL detector, excitation at 445 nm, emission at 535 nm). The peptide concentrations in the plasma samples were determined by integrating the area under the intact peptide peak (ChemStation software, Agilent Technologies) and calculating the concentration using a standard curve derived from a dilution series of known peptide concentrations in mouse plasma analyzed with the same protocol. Pharmacokinetic parameters were calculated based on a two-compartment model.

Fluorescence imaging of mice

Prior to injection, the ventral fur of mice was shaved off with a surgery prep shaver under anesthesia. Mice were IV injected with KLK5 inhibitor (KLK5(1)-tag; 6.2 mg/kg) or equimolar doses (2 µmol/kg) of peptide-fluorescein conjugate (KLK5(1)-fluorescein;

3.2 mg/kg) as described above. One mouse was injected with 100 μL PBS as control to measure fluorescence background derived from the mice. Mice were imaged using a CCD camera (IVIS Spectrum, PerkinElmer, USA; excitation filter: 495 nm, emission filter: 519 nm) at the indicated time points. All imaging data were processed using the Living Image software (PerkinElmer, USA) taking the shaved ventral region as region of interest (ROI) and plotting the average radiant efficiency. For imaging the fluorescence of skin samples and visceral organs, mice were IP injected with 12.4 mg/kg KLK5 inhibitor (KLK5(1)-tag), euthanized by cervical dislocation 48 hrs after injection, and organs were harvested and imaged as described above.

Fluorescence microscopy of skin

Mice were IP injected with KLK5(1)-tag (6.4 mg/kg; 2 μmol/kg) in 200 μL injection buffer. Mice were sacrificed 8 hrs after injection by cervical dislocation. 1 cm² patches of ventral skin were taken and fixed by embedding in cryomatrix and freezing using isopentane cooled down with dry ice. Samples were stored at -20 °C and microscopy sides were prepared by the EPFL Histology core facility (Dr. Jessica Sordet-Dessimoz). The skin samples were cut into 10 μm sections using a cryostat (Leica CM3050S). Sections were directly mounted on Superfrost+ slides (Menzel Gläser) and slides were stored at -20 °C until staining. DAPI staining was performed as following: slides were air dried for 30 min at RT, stained for 10 min in DAPI solution (diluted 1 : 10,000 in PBS from a 1 mg/mL stock solution in water), washed three times for 5 min with PBS and mounted using Fluoromount-G mounting medium. Fluorescence microscopy was conducted at the EPFL Bioimaging and Optics Platform (Dr. Arne Seitz) on a slide scanner (Olympus VS120-L100, 20x UPLSAPO objective, DAPI and Cy5 channel settings) using consistent illumination times for all samples. Images were analyzed using QuPath software setting identical contrast and brightness scales for all samples. Intensity profiles were generated using ImageJ software and plotted with GraphPad Prism.

ANCILLARY INFORMATION

Supporting Information Availability

The Supporting Information is available free of charge at https://pubs.acs.org/doi/xyz

Expression of human KLK5 and KLK7 and activity (Figure S1); HPLC chromatograms of bicyclic and monocyclic peptides (Figure S2); specificity profiling of KLK5(1) inhibitor (Figure S3); HPLC chromatograms of peptides containing unnatural amino acids (Figure S4); activity and SAR data of peptides containing unnatural amino acids (Figure S5); synthesis strategy for KLK inhibitors with albumin-binding tag (Figure S6); KLK inhibition curves and FP albumin binding of inhibitor-tag conjugates (Figure S7); LC-MS data of stability assays of peptides and peptide conjugates in human plasma (Figure S8); LC-MS data of stability assays of engineered KLK7 inhibitor (Figure S9); chemical structures of KLK5(1)-tag and KLK7(5)-tag (Figure S10); RP-HPLC analysis of inhibitor conjugates in blood samples (Figure S11); chemical structure of KLK5(1)-SiR-tag (Figure S12); skin sections showing distribution of KLK5(1)-SiR-tag in mouse skin (Figure S13).

Corresponding Author Information

Christian Heinis

christian.heinis@epfl.ch

Abbreviations Used

BBMP, 2,6-bis(bromomethyl)pyridine; DBA, 1,3-dibromoacetone; IMAC, metal affinity chromatography; KLK5, kallikrein-related peptidase 5; KLK7, kallikrein-related peptidase 7; KLK14, kallikrein-related peptidase 14; LEKTI, lympho-epithelial Kazal-type related inhibitor; NS, Netherton syndrome; PAR2, protease-activated receptor 2; SFTI-1, sunflower trypsin inhibitor**;** SPINK5, serine peptidase inhibitor Kazal-type 5

Acknowledgments

We thank David Hacker for help with the recombinant expression of the KLKs, Jessica Sordet-Dessimoz for help with preparing tissue sections and Thierry Laroche for help with microscopy. The project was kindly supported by the Swiss National Science Foundation (SNSF grant 166929; ERA-NET E-Rare-3: Netherton syndrome; from mechanisms to therapies – KLKIN). This project has received funding from the European Union's Horizon 2020 research and innovation program under the ERA-NET Cofund action N° 643578.

.

Competing Interests

P.G., A.Z., C.H. and A.H. are inventors of a patent. The other authors declare no competing financial interests.

REFERENCES

(1) Egelrud, T.; Brattsand, M.; Kreutzmann, P.; Walden, M.; Vitzithum, K.; Marx, U. C.; Forssmann, W. G.; Magert, H. J. HK5 and HK7, Two Serine Proteinases Abundant in Human Skin, Are Inhibited by LEKTI Domain 6. *Br. J. Dermatol.* **2005**, *153* (6), 1200–1203.

(2) Chavanas, S.; Bodemer, C.; Rochat, A.; Hamel-Teillac, D.; Ali, M.; Irvine, A. D.; Bonafé, J.-L.; Wilkinson, J.; Taïeb, A.; Barrandon, Y.; Harper, J. I.; de Prost, Y.; Hovnanian, A. Mutations in SPINK5, Encoding a Serine Protease Inhibitor, Cause Netherton Syndrome. *Nat. Genet.* **2000**, *25* (2), 141–142.

(3) Petrova, E.; Hovnanian, A. Advances in Understanding of Netherton Syndrome and Therapeutic Implications. *Expert Opin. Orphan Drugs* **2020**, *8* (11), 455–487.

(4) Kasparek, P.; Ileninova, Z.; Zbodakova, O.; Kanchev, I.; Benada, O.; Chalupsky, K.; Brattsand, M.; Beck, I. M.; Sedlacek, R. KLK5 and KLK7 Ablation Fully Rescues Lethality of Netherton Syndrome-Like Phenotype. *PLOS Genet.* **2017**, *13* (1), e1006566.

(5) Furio, L.; Pampalakis, G.; Michael, I. P.; Nagy, A.; Sotiropoulou, G.; Hovnanian, A. KLK5 Inactivation Reverses Cutaneous Hallmarks of Netherton Syndrome. *PLOS Genet.* **2015**, *11* (9), e1005389.

(6) Prassas, I.; Eissa, A.; Poda, G.; Diamandis, E. P. Unleashing the Therapeutic Potential of Human Kallikrein-Related Serine Proteases. *Nat. Rev. Drug Discov.* **2015**, *14* (3), 183–202.

(7) Sotiropoulou, G.; Pampalakis, G. Targeting the Kallikrein-Related Peptidases for Drug Development. *Trends Pharmacol. Sci.* **2012**, *33* (12), 623–634.

(8) Deraison, C.; Bonnart, C.; Lopez, F.; Besson, C.; Robinson, R.; Jayakumar, A.; Wagberg, F.; Brattsand, M.; Hachem, J. P.; Leonardsson, G.; Hovnanian, A. LEKTI Fragments Specifically Inhibit KLK5, KLK7, and KLK14 and Control Desquamation through a PH-Dependent Interaction. *Mol. Biol. Cell* **2007**, *18* (9),

3607–3619.

(9) Chen, W.; Kinsler, V. A.; Macmillan, D.; Di, W.-L. Tissue Kallikrein Inhibitors Based on the Sunflower Trypsin Inhibitor Scaffold – A Potential Therapeutic Intervention for Skin Diseases. *PLoS One* **2016**, *11* (11), e0166268.

(10) de Veer, S. J.; Swedberg, J. E.; Akcan, M.; Rosengren, K. J.; Brattsand, M.; Craik, D. J.; Harris, J. M. Engineered Protease Inhibitors Based on Sunflower Trypsin Inhibitor-1 (SFTI-1) Provide Insights into the Role of Sequence and Conformation in Laskowski Mechanism Inhibition. *Biochem. J.* **2015**, *469* (2), 243–253.

(11) de Veer, S. J.; Furio, L.; Swedberg, J. E.; Munro, C. A.; Brattsand, M.; Clements, J. A.; Hovnanian, A.; Harris, J. M. Selective Substrates and Inhibitors for Kallikrein-Related Peptidase 7 (KLK7) Shed Light on KLK Proteolytic Activity in the Stratum Corneum. *J. Invest. Dermatol.* **2017**, *137* (2), 430–439.

(12) de Veer, S. J.; Swedberg, J. E.; Brattsand, M.; Clements, J. A.; Harris, J. M. Exploring the Active Site Binding Specificity of Kallikrein-Related Peptidase 5 (KLK5) Guides the Design of New Peptide Substrates and Inhibitors. *Biol. Chem.* **2016**, *397* (12), 1237–1249.

(13) Li, C. Y.; de Veer, S. J.; White, A. M.; Chen, X.; Harris, J. M.; Swedberg, J. E.; Craik, D. J. Amino Acid Scanning at P5′ within the Bowman–Birk Inhibitory Loop Reveals Specificity Trends for Diverse Serine Proteases. *J. Med. Chem.* **2019**, *62* (7), 3696–3706.

(14) Krastel, P.; Liechty, B.-M. Meingassner, J. G.; Shmitt, E.; Schreiner, E. P. Cyclic Depsipeptides. US 2009/0156472 A1, 2009.

(15) Hoelz, L. V. B.; Zorzanelli, B. C.; Azevedo, P. H. R. d. A.; Passos, S. G.; de Souza, L. R.; Zani, M.; Pinheiro, S.; Puzer, L.; Dias, L. R. S.; Muri, E. M. F. Synthesis, Biological Evaluation and Molecular Modeling of Pseudo-Peptides Based Statine as Inhibitors for Human Tissue Kallikrein 5. *Eur. J. Med. Chem.* **2016**, *112*, 39–47.

(16) Walker, A. L.; Bingham, R. P.; Edgar, E. V.; Ferrie, A.; Holmes, D. S.; Liddle, J.; Polyakova, O.; Rella, M.; Smith, K. J.; Thorpe, J. H.; Wang, Y.; White, G. V.; Young, R. J.; Hovnanian, A. Structure Guided Drug Design to Develop Kallikrein 5 Inhibitors to Treat Netherton Syndrome. *Bioorg. Med. Chem. Lett.* **2019**, *29* (12), 1454–1458.

(17) White, G. V.; Edgar, E. V.; Holmes, D. S.; Lewell, X. Q.; Liddle, J.; Polyakova, O.; Smith, K. J.; Thorpe, J. H.; Walker, A. L.; Wang, Y.; Young, R. J.; Hovnanian, A. Kallikrein 5 Inhibitors Identified through Structure Based Drug Design in Search for a Treatment for Netherton Syndrome. *Bioorg. Med. Chem. Lett.* **2019**, *29* (6), 821–825.

(18) Liddle, J.; Beneton, V.; Benson, M.; Bingham, R.; Bouillot, A.; Boullay, A.-B.; Brook, E.; Cryan, J.; Denis, A.; Edgar, E.; Ferrie, A.; Fouchet, M.-H.; Grillot, D.; Holmes, D. S.; Howes, A.; Krysa, G.; Laroze, A.; Lennon, M.; McClure, F.; Moquette, A.; Nicodeme, E.; Santiago, B.; Santos, L.; Smith, K. J.; Thorpe, J. H.; Thripp, G.; Trottet, L.; Walker, A. L.; Ward, S. A.; Wang, Y.; Wilson, S.; Pearce, A. C.; Hovnanian, A. A Potent and Selective Kallikrein-5 Inhibitor Delivers High Pharmacological Activity in Skin from Patients with Netherton Syndrome. *J. Invest. Dermatol.* **2021**, *141* (9), 2272–2279.

(19) Tan, X.; Soualmia, F.; Furio, L.; Renard, J.-F.; Kempen, I.; Qin, L.; Pagano, M.; Pirotte, B.; El Amri, C.; Hovnanian, A.; Reboud-Ravaux, M. Toward the First Class of Suicide Inhibitors of Kallikreins Involved in Skin Diseases. *J. Med. Chem.* **2015**, *58* (2), 598–612.

(20) Oliveira, J. P. C.; Freitas, R. F.; Melo, L. S. de; Barros, T. G.; Santos, J. A. N.; Juliano, M. A.; Pinheiro, S.; Blaber, M.; Juliano, L.; Muri, E. M. F.; Puzer, L. Isomannide-Based Peptidomimetics as Inhibitors for Human Tissue Kallikreins 5 and 7. *ACS Med. Chem. Lett.* **2014**, *5* (2), 128–132.

(21) Flohr, S.; Randl, S.A. Ostermann, N. Hassiepen, U.; Berst, F.; Bodendorf, U. Gerhartz, B.; Marzinzik, A.; Ehrhardt, C.; Meingassner, J. G. Kallikrein 7

Modulators. WO 2009/000878 A1, 2008.

(22) Carle, V.; Kong, X.-D.; Comberlato, A.; Edwards, C.; Díaz-Perlas, C.; Heinis, C. Generation of a 100-Billion Cyclic Peptide Phage Display Library Having a High Skeletal Diversity. *Protein Eng. Des. Sel.* **2021**, *34*.

(23) Angelini, A.; Cendron, L.; Chen, S.; Touati, J.; Winter, G.; Zanotti, G.; Heinis, C. Bicyclic Peptide Inhibitor Reveals Large Contact Interface with a Protease Target. *ACS Chem. Biol.* **2012**, *7* (5), 817–821.

(24) Baeriswyl, V.; Rapley, H.; Pollaro, L.; Stace, C.; Teufel, D.; Walker, E.; Chen, S.; Winter, G.; Tite, J.; Heinis, C. Bicyclic Peptides with Optimized Ring Size Inhibit Human Plasma Kallikrein and Its Orthologues While Sparing Paralogous Proteases. *ChemMedChem* **2012**, *7* (7), 1173–1176.

(25) Pollaro, L.; Heinis, C. Strategies to Prolong the Plasma Residence Time of Peptide Drugs. *Medchemcomm* **2010**, *1* (5), 319–324.

(26) Angelini, A.; Morales-Sanfrutos, J.; Diderich, P.; Chen, S.; Heinis, C. Bicyclization and Tethering to Albumin Yields Long-Acting Peptide Antagonists. *J. Med. Chem.* **2012**, *55* (22), 10187–10197.

(27) Zorzi, A.; Middendorp, S. J.; Wilbs, J.; Deyle, K.; Heinis, C. Acylated Heptapeptide Binds Albumin with High Affinity and Application as Tag Furnishes Long-Acting Peptides. *Nat. Commun.* **2017**, *8* (1), 16092.

(28) Dennis, M. S.; Zhang, M.; Meng, Y. G.; Kadkhodayan, M.; Kirchhofer, D.; Combs, D.; Damico, L. A. Albumin Binding as a General Strategy for Improving the Pharmacokinetics of Proteins. *J. Biol. Chem.* **2002**, *277* (38), 35035–35043.

(29) Pollaro, L.; Raghunathan, S.; Morales-Sanfrutos, J.; Angelini, A.; Kontos, S.; Heinis, C. Bicyclic Peptides Conjugated to an Albumin-Binding Tag Diffuse Efficiently into Solid Tumors. *Mol. Cancer Ther.* **2015**, *14* (1), 151–161.

(30) Rajendra, Y.; Kiseljak, D.; Baldi, L.; Hacker, D. L.; Wurm, F. M. A Simple High-Yielding Process for Transient Gene Expression in CHO Cells. *J. Biotechnol.*

2011, *153* (1–2), 22–26.

(31) Schechter, N. M.; Choi, E.-J.; Wang, Z.-M.; Hanakawa, Y.; Stanley, J. R.; Kang, Y.; Clayman, G. L.; Jayakumar, A. Inhibition of Human Kallikreins 5 and 7 by the Serine Protease Inhibitor Lympho-Epithelial Kazal-Type Inhibitor (LEKTI). *Biol. Chem.* **2005**, *386* (11), 1173–1184.

(32) Rentero Rebollo, I.; Heinis, C. Phage Selection of Bicyclic Peptides. *Methods* **2013**, *60* (1), 46–54.

(33) Abbenante, J.; Leung, D.; Bond, T. J.; Fairlie, D. P. An Efficient Fmoc Strategy for the Rapid Synthesis of Peptide Para-Nitroanilides. *Lett. Pept. Sci.* **2000**, *7* (6), 347–351.

TABLE OF CONTENTS GRAPHIC

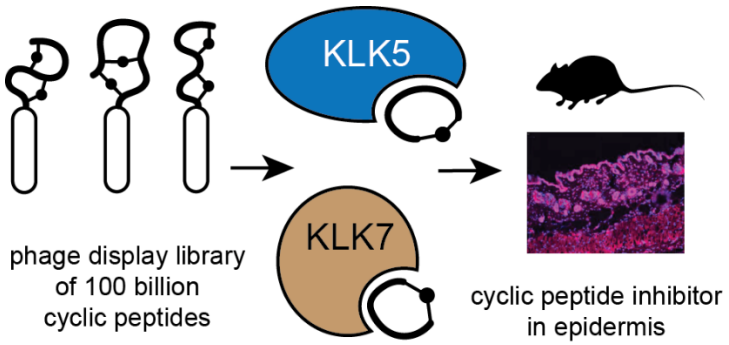

Supporting Information

Phage display selected cyclic peptide inhibitors of kallikrein-related peptidases 5 and 7 and their in vivo delivery to skin

Patrick Gonschorek[1], Alessandro Zorzi[1], Tamara Maric[1], Mathilde Le Jeune[1], Mischa Schüttel[1], Mathilde Montagnon[1], Rebeca Gómez-Ojea[1], Denis Patrick Vollmar[1], Chantal Whitfield[1], Luc Reymond[2], Vanessa Carle[1], Hitesh Verma[1], Oliver Schilling[3], Alain Hovnanian[4] and Christian Heinis[1,*]

[1]Institute of Chemical Sciences and Engineering, School of Basic Sciences, Ecole Polytechnique Fédérale de Lausanne (EPFL), CH-1015 Lausanne, Switzerland

[2]Biomolecular Screening Facility, Swiss Federal Institute of Technology Lausanne (EPFL), CH-1015 Lausanne, Switzerland

[3]Institute for Surgical Pathology, Medical Center, Faculty of Medicine, University of Freiburg, Freiburg 79106, Germany

[4]INSERM UMR1163, Imagine Institute, University of Paris, Paris, France; Department of Genetics, Necker Hospital for Sick Children (AP-HP), Paris 75015, France

*Correspondence should be addressed to Christian Heinis (christian.heinis@epfl.ch)

Contents

Supplementary Figures

Supplementary Figures

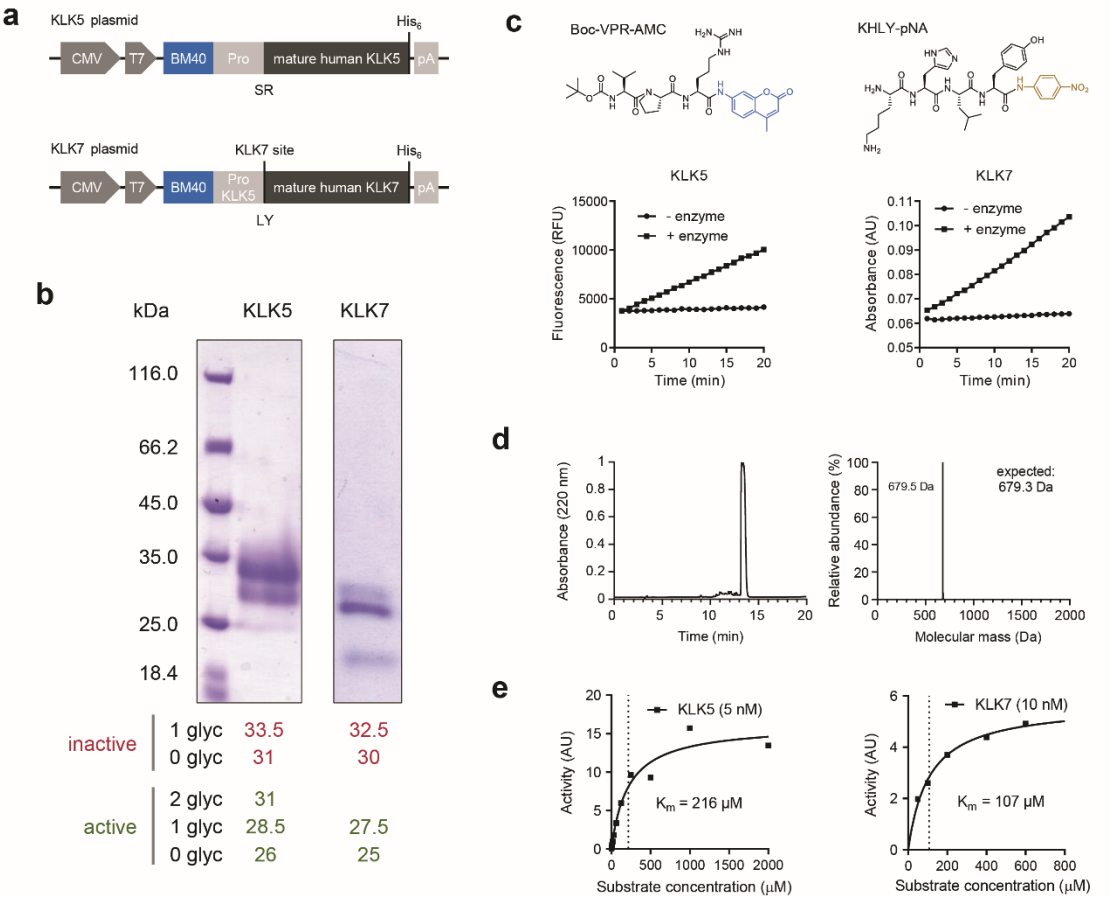

Figure S1. Recombinant expression of human KLK5 and KLK7 and their hydrolytic activity. a, DNA vectors cloned for expression of the proteases in mammalian cells. b, SDS-PAGE analysis of proteins after purification by immobilized metal affinity chromatography. The numbers below indicate the expected molecular weights for the proteases with (red) or without pro-domain (green), and with or without glycosylation. c, Activity of enzymes tested with the indicated fluorogenic or chromogenic substrates. d, HPLC and MS analysis of chromogenic KHLY-pNA substrate. e, Determination of Michaelis-Menten constants for both protease/substrate pairs.

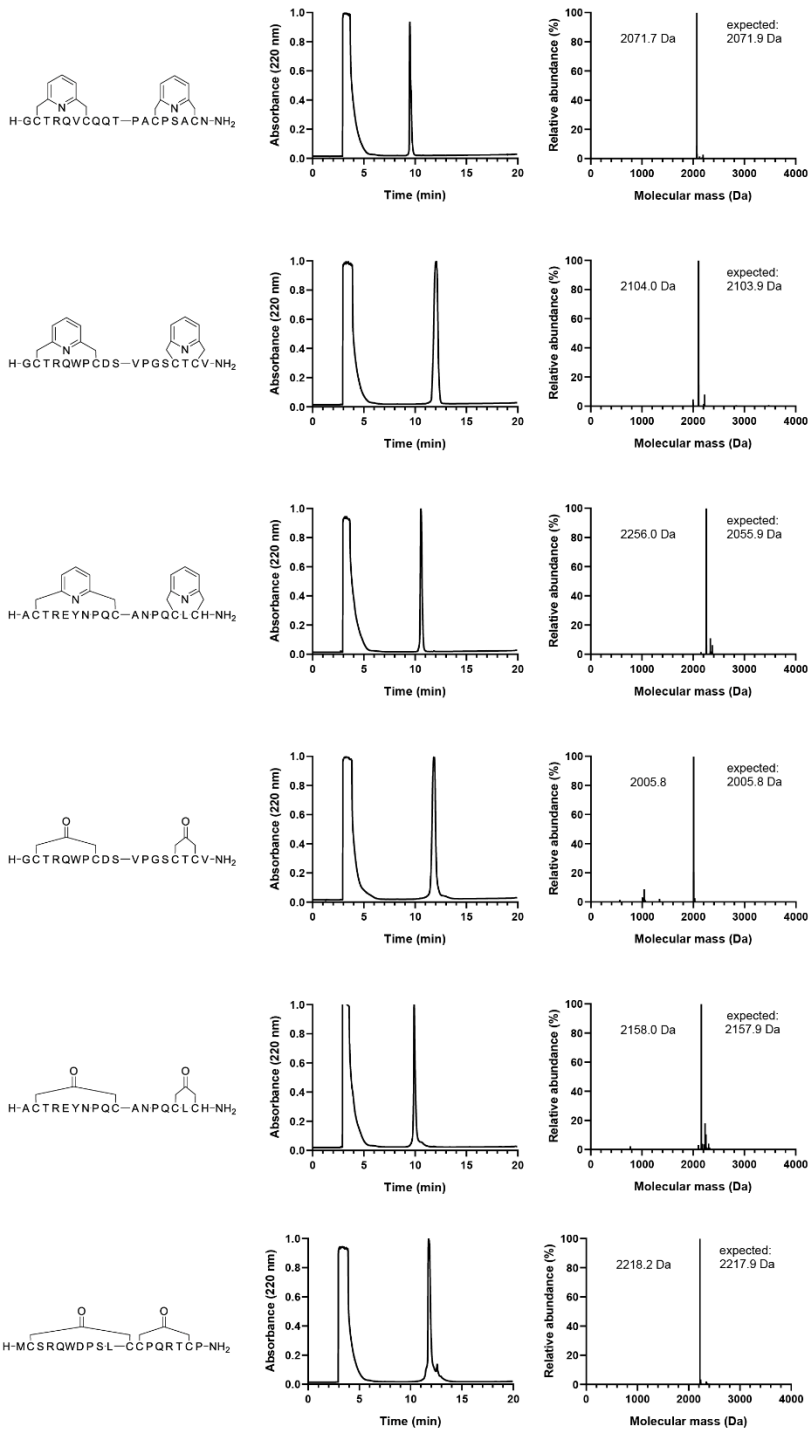

Figure S2. Purity and identity of bicyclic and monocyclic peptides. Analytical HPLC chromatograms and deconvoluted MS spectra of cyclic peptides. The molecular masses of the most abundant isotope are indicated as “expected” values.

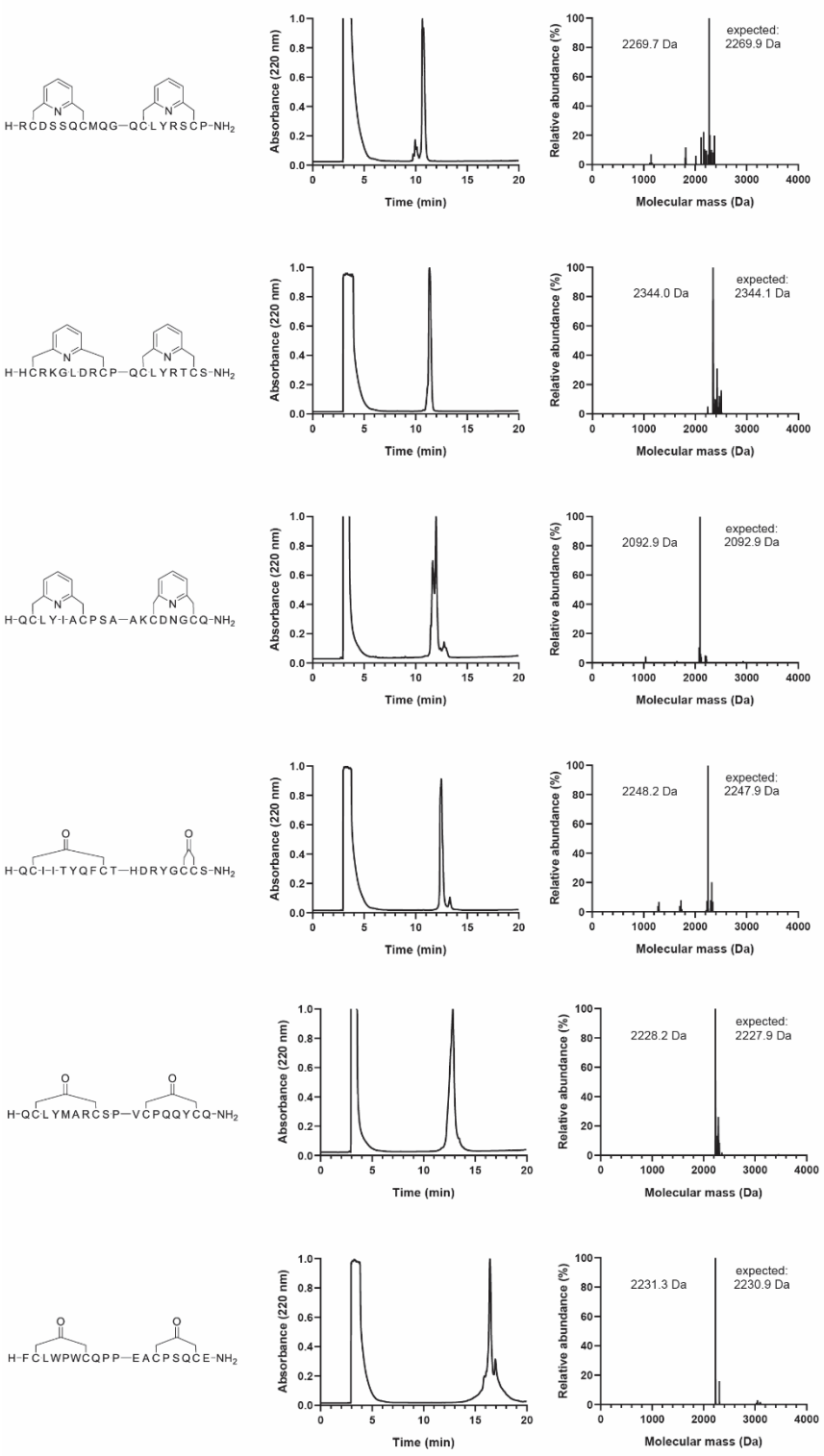

Figure S2. Continued

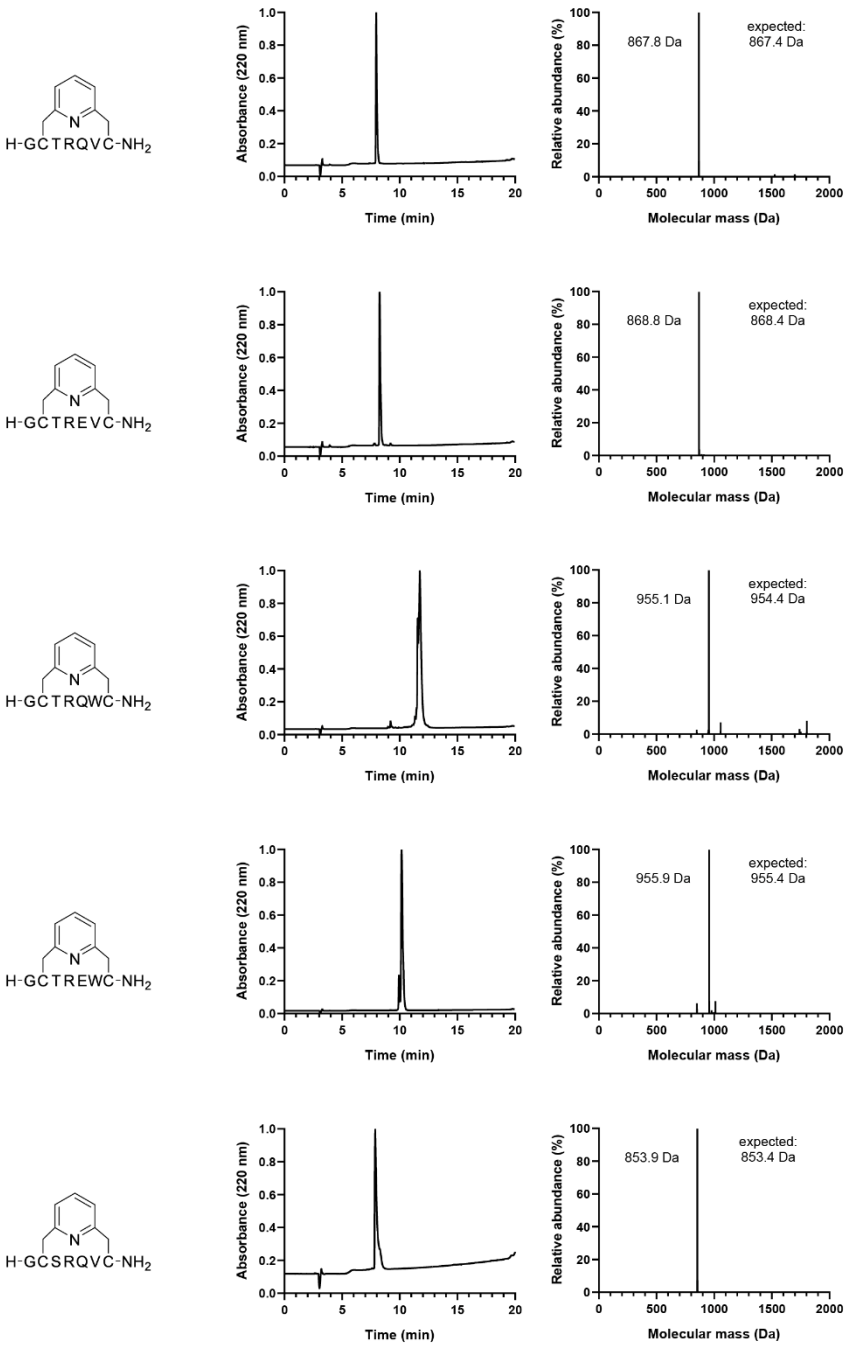

Figure S2. Continued

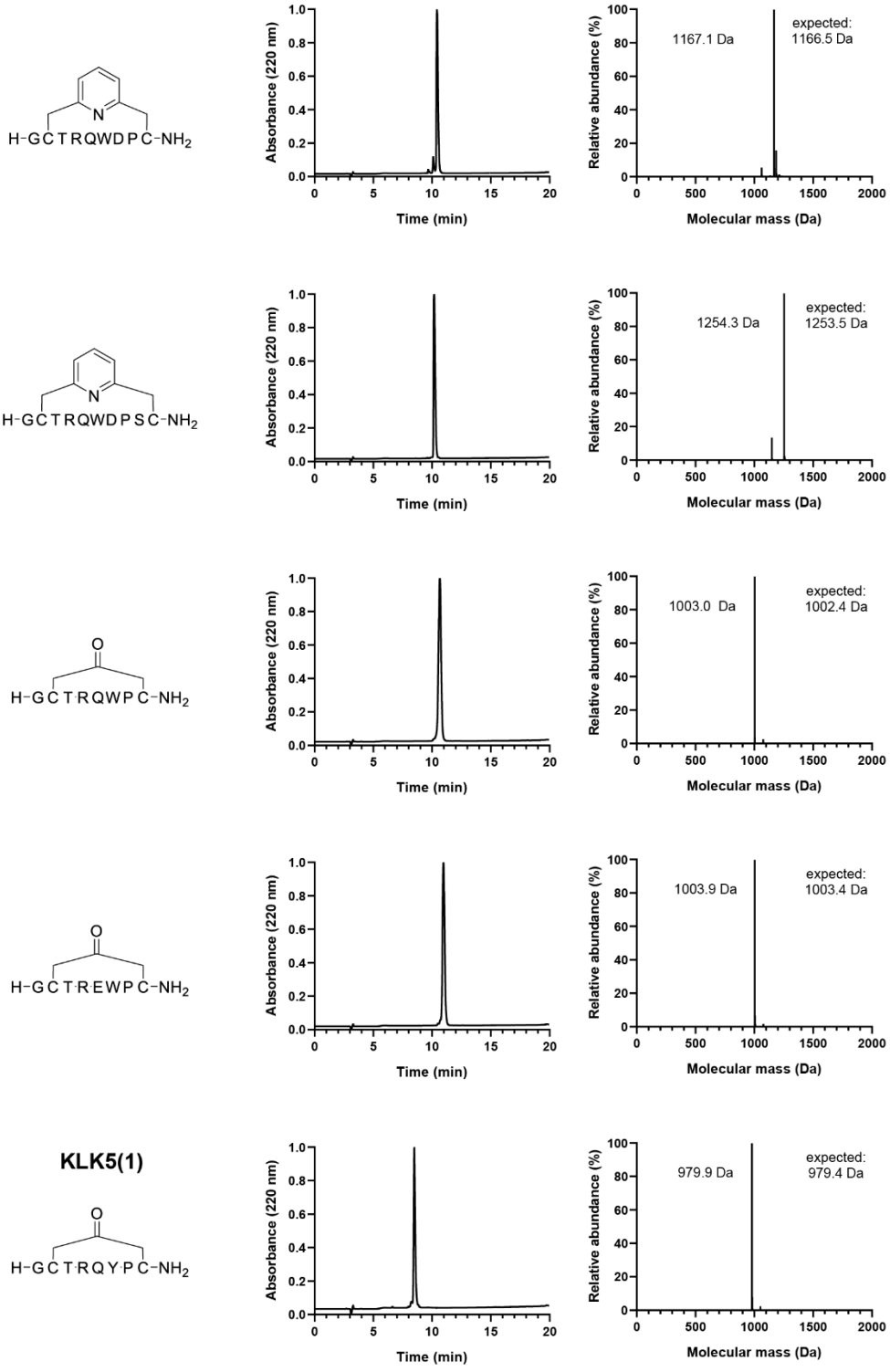

Figure S2. Continued

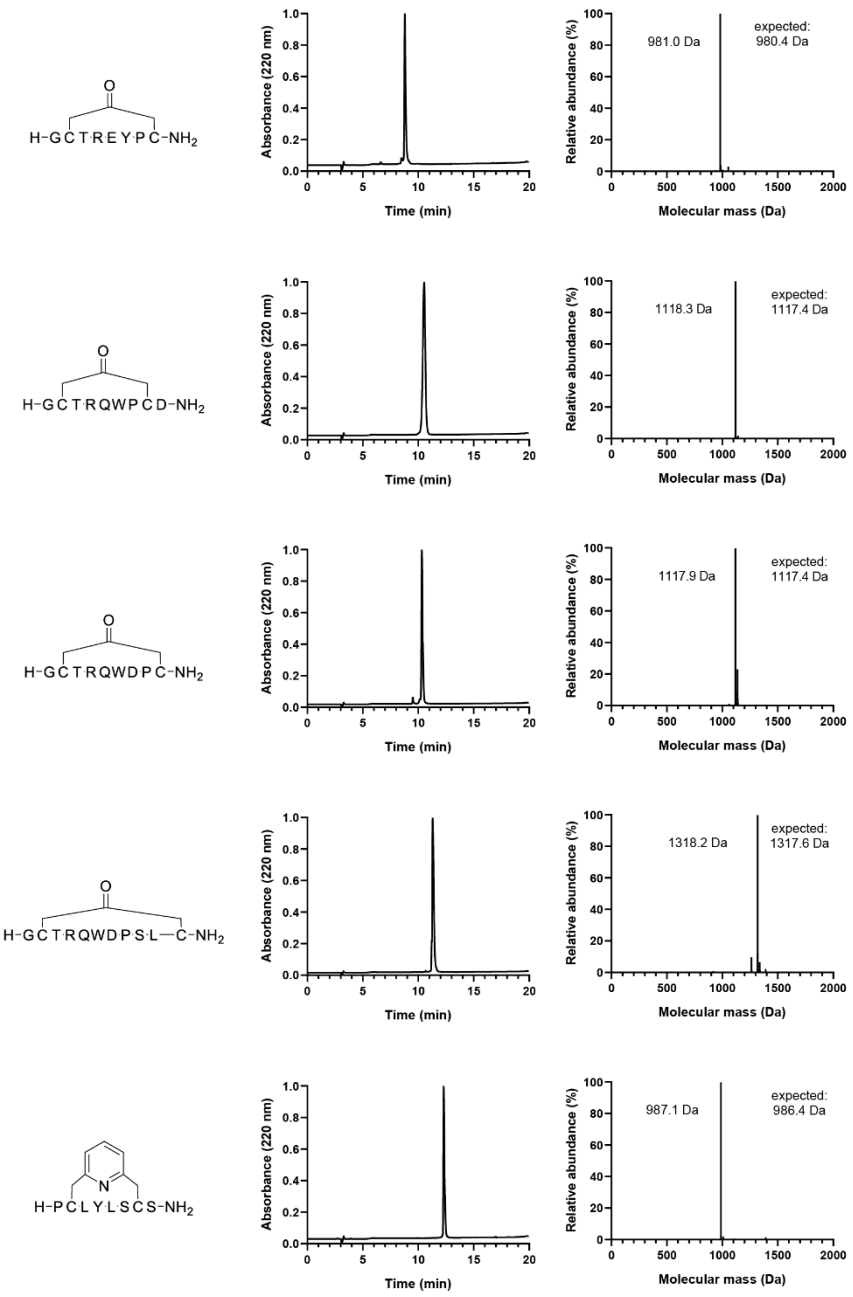

Figure S2. Continued

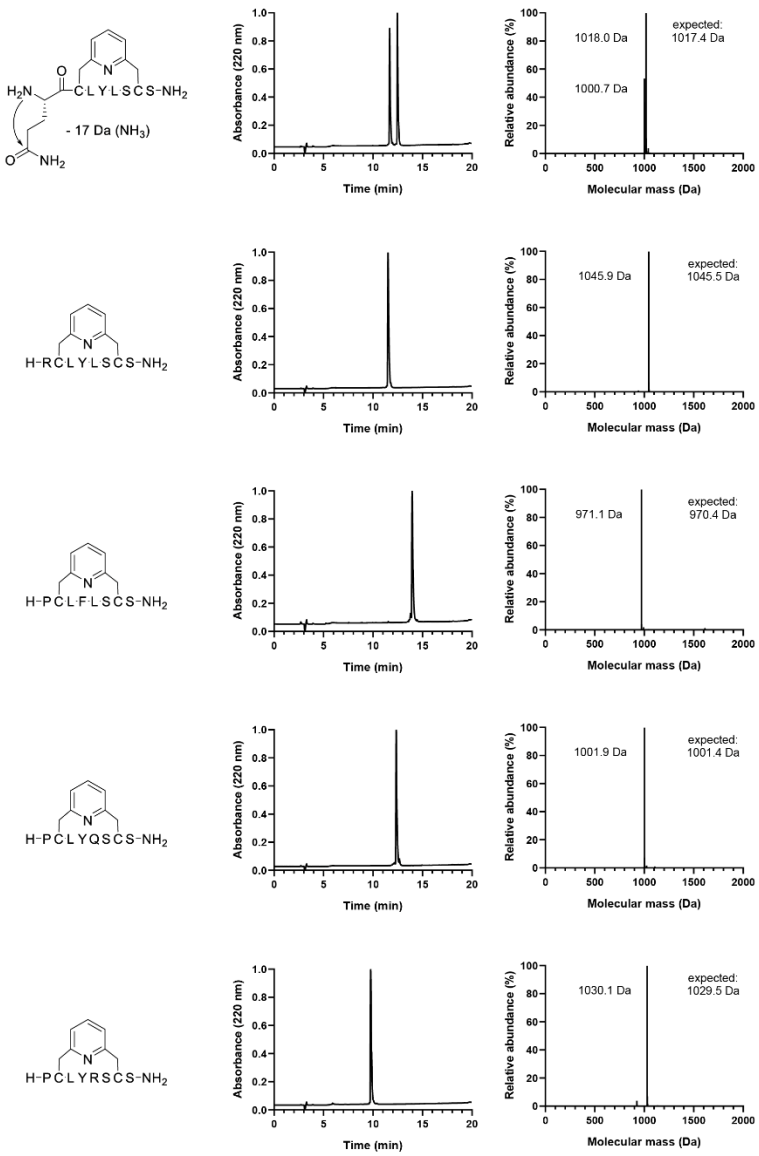

Figure S2. Continued

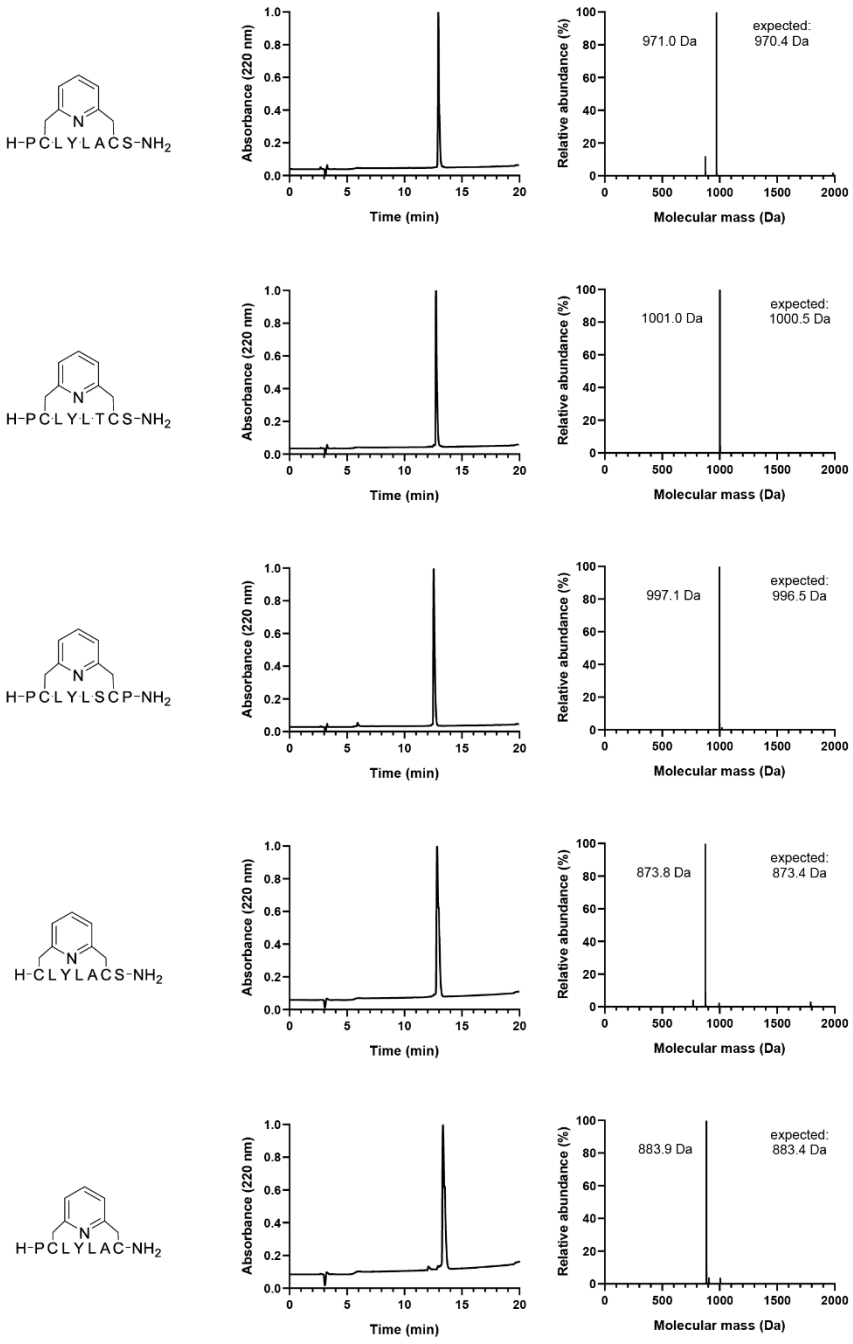

Figure S2. Continued

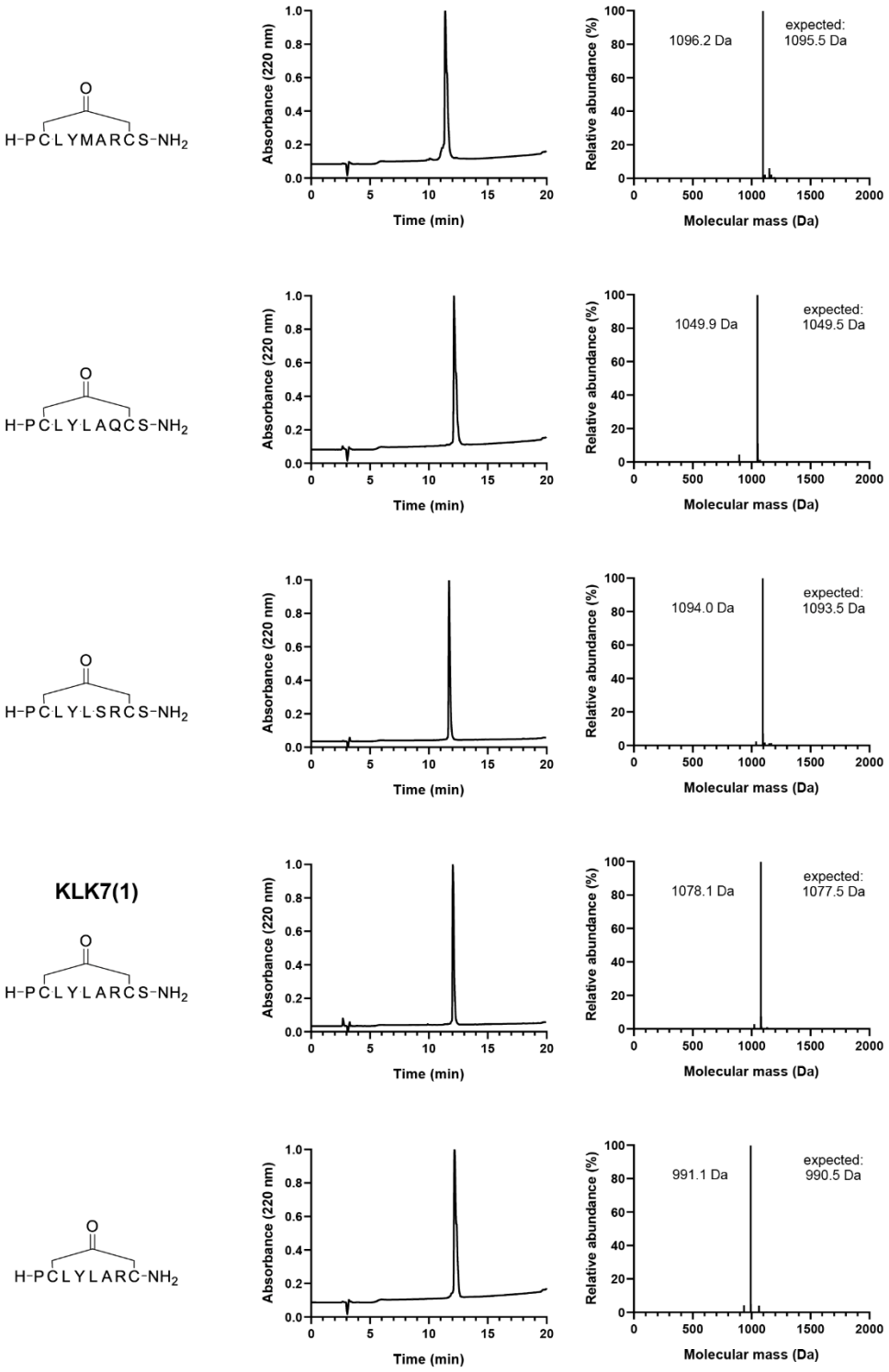

Figure S2. Continued

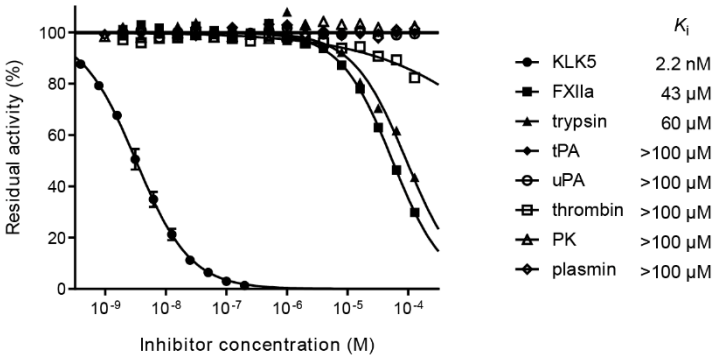

Figure S3. Specificity profiling of KLK5 inhibitor KLK5(1). KLK5 and seven other trypsin-like serine proteases were incubated with the indicated concentrations of KLK5(1) and the residual protease activity measured in activity assays using fluorogenic protease substrates.

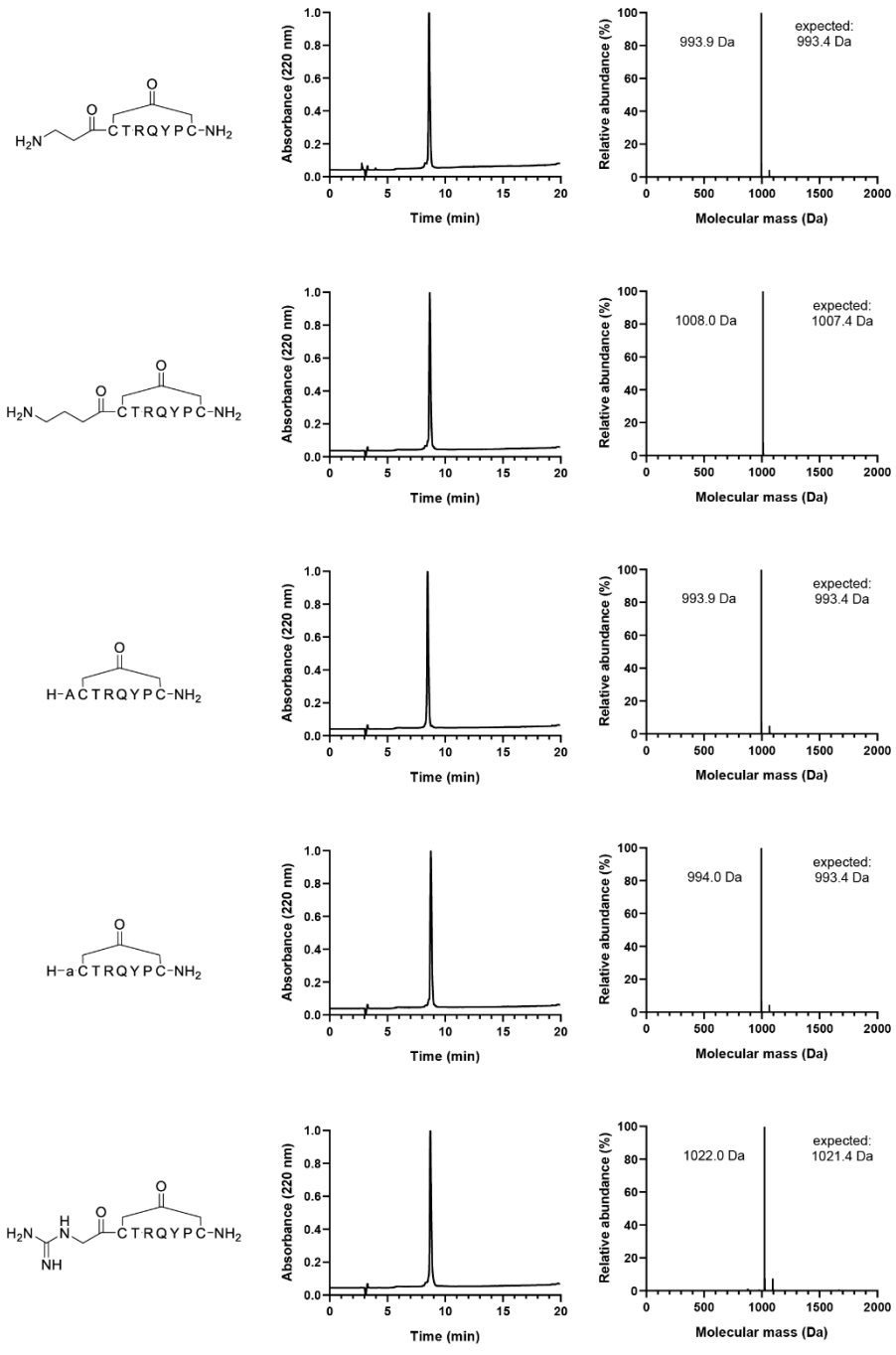

Figure S4. Purity and identity of peptides containing unnatural amino acids. Analytical HPLC chromatograms and MS spectra of cyclic peptides. The expected and experimentally observed molecular weights are indicated.

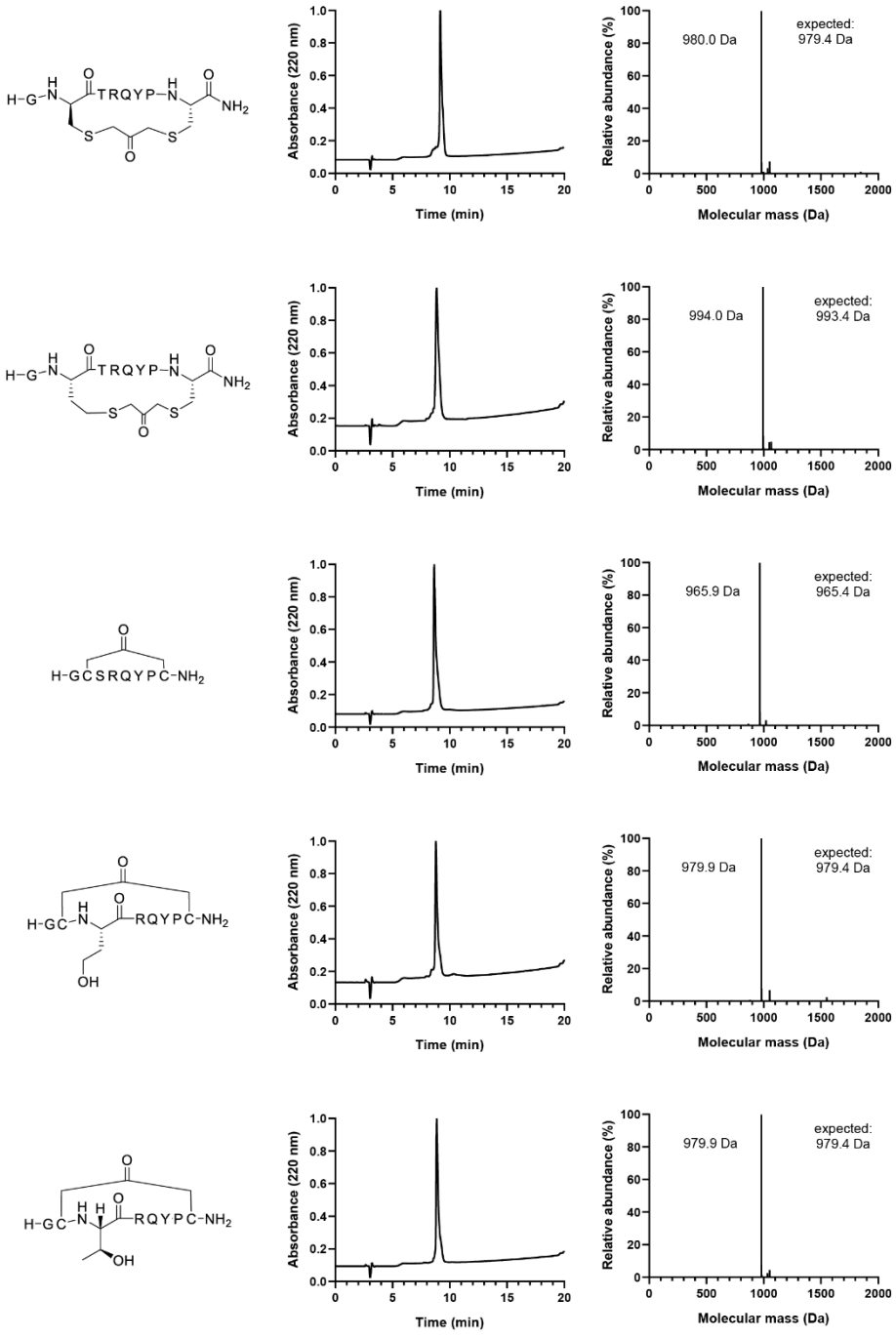

Figure S4. Continued

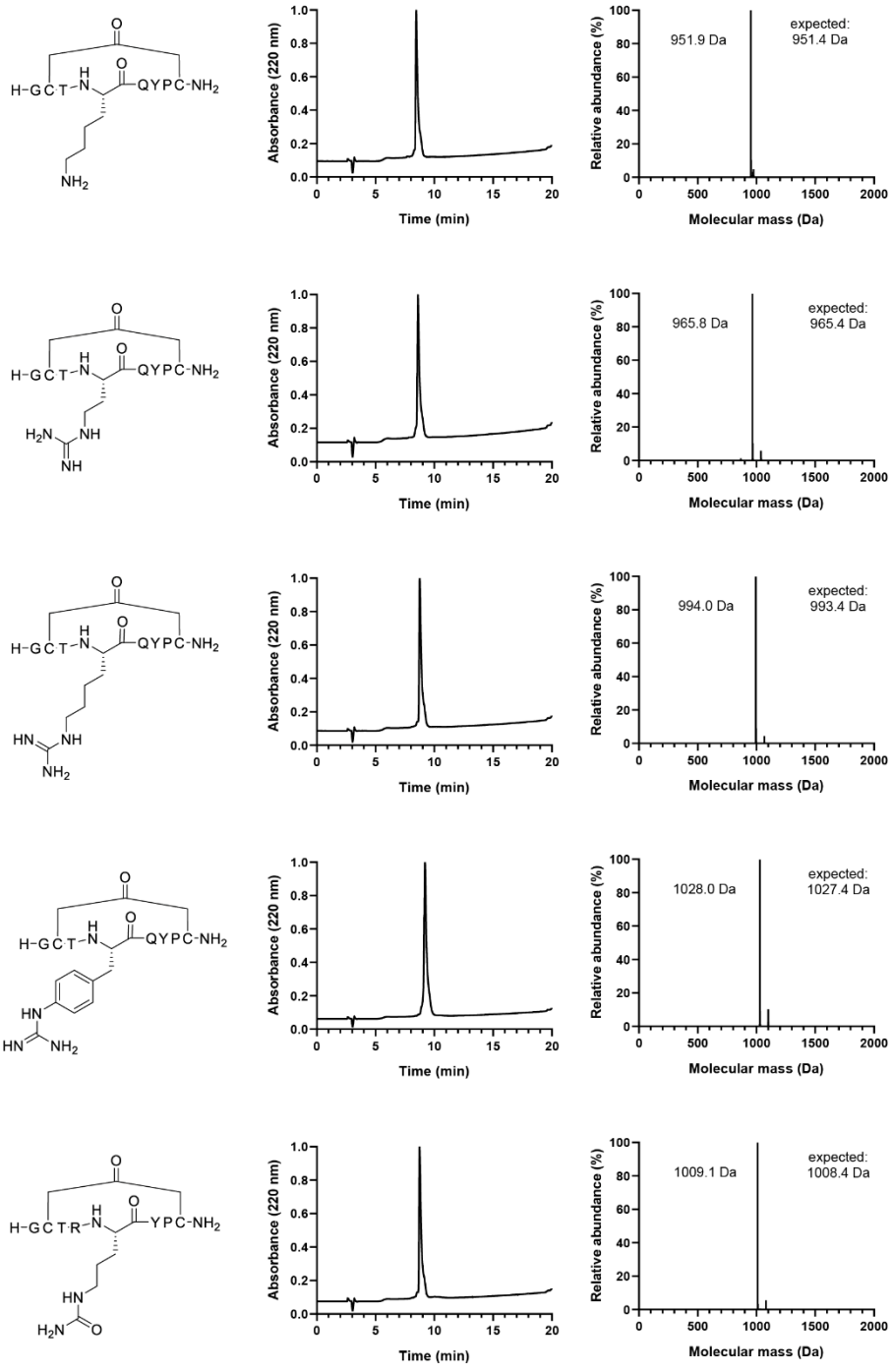

Figure S4. Continued

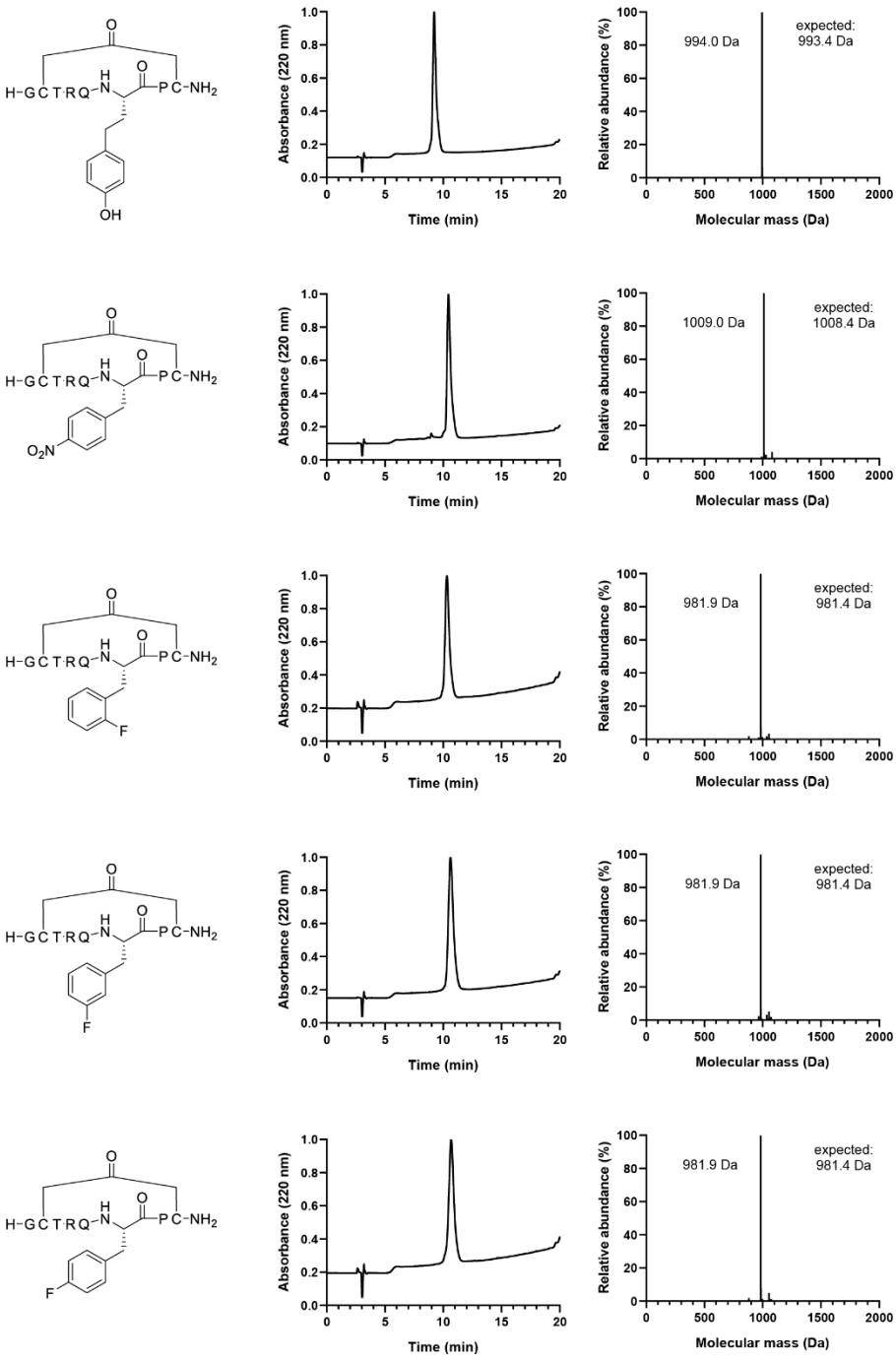

Figure S4. Continued

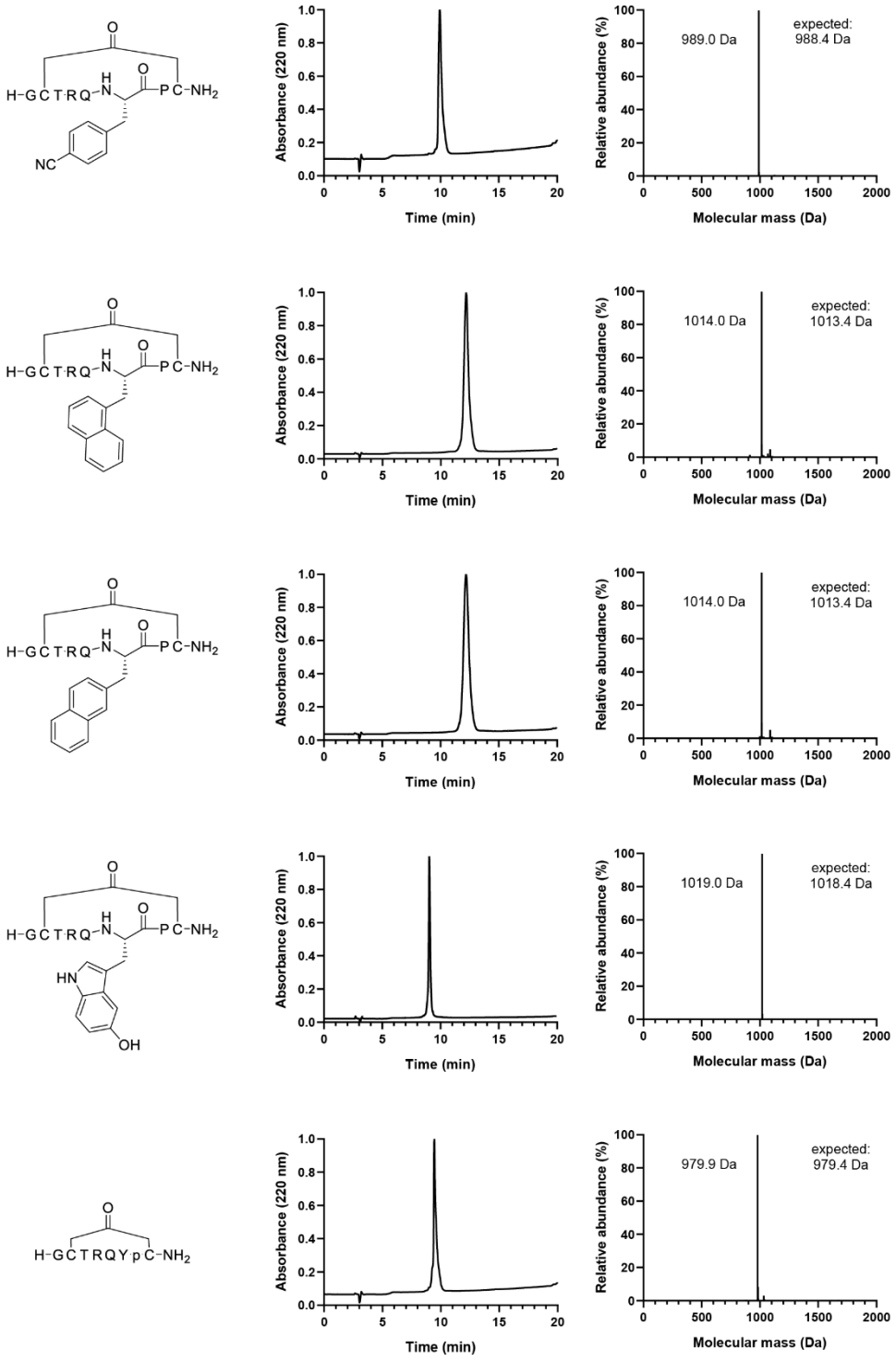

Figure S4. Continued

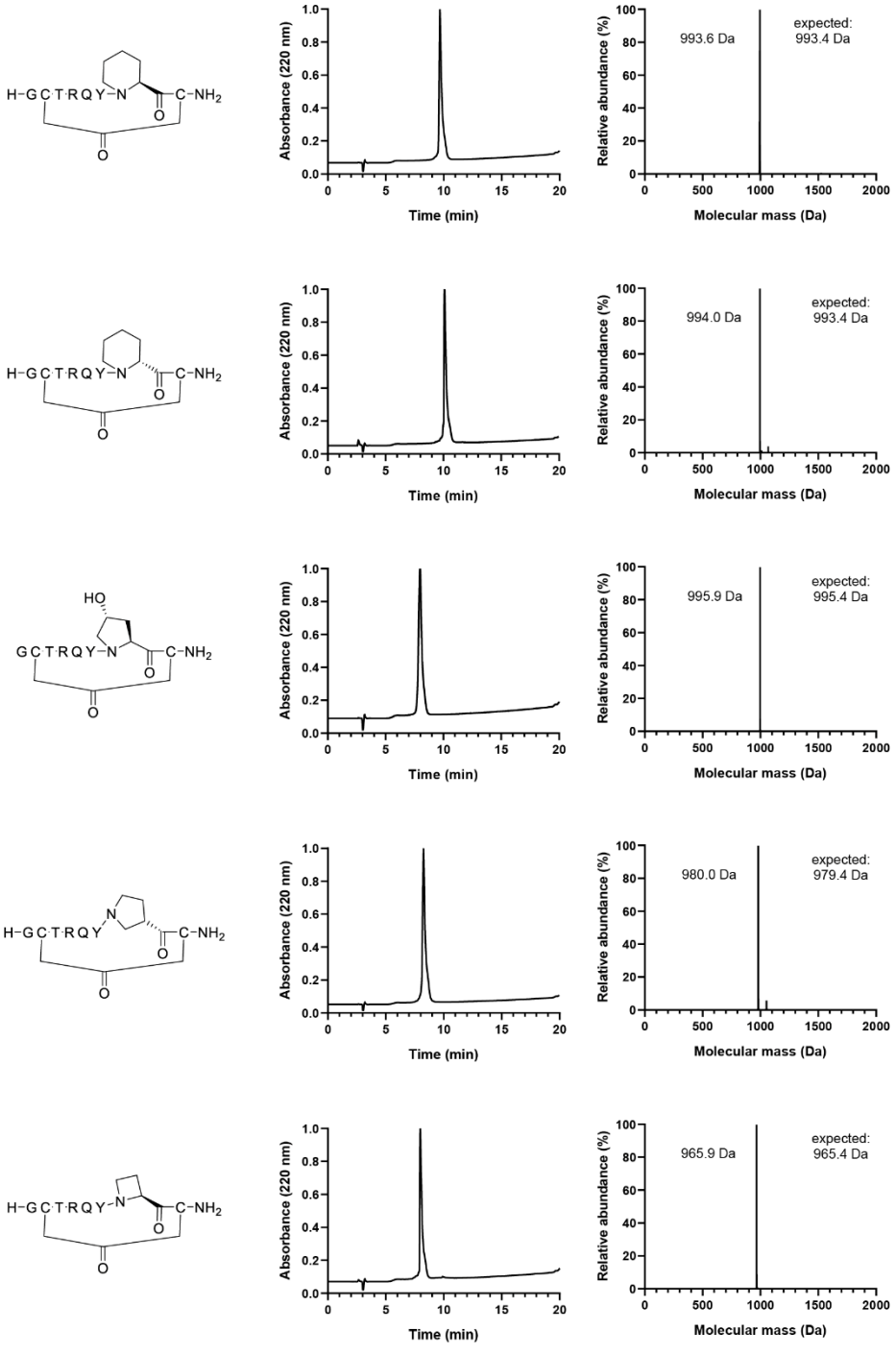

Figure S4. Continued

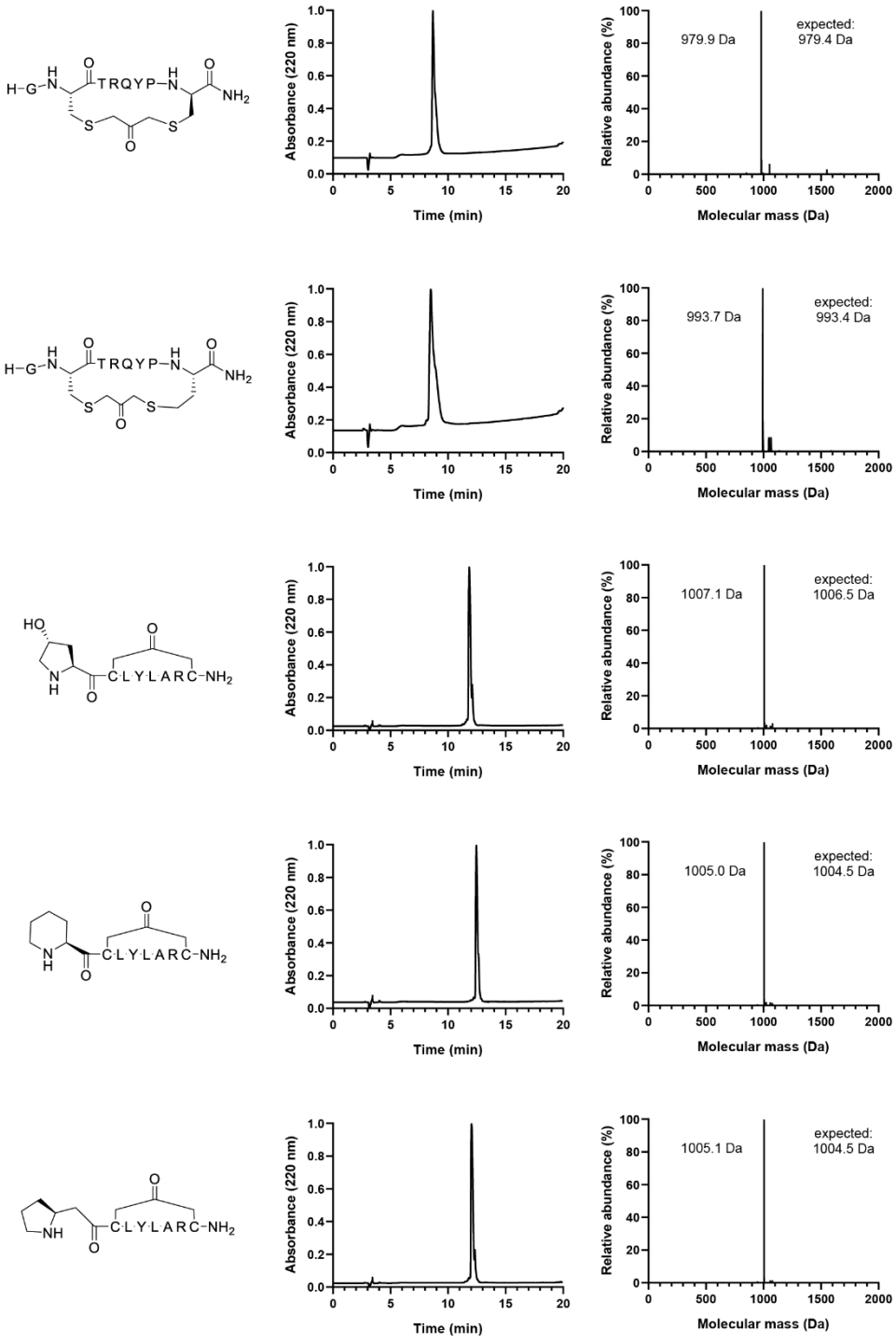

Figure S4. Continued

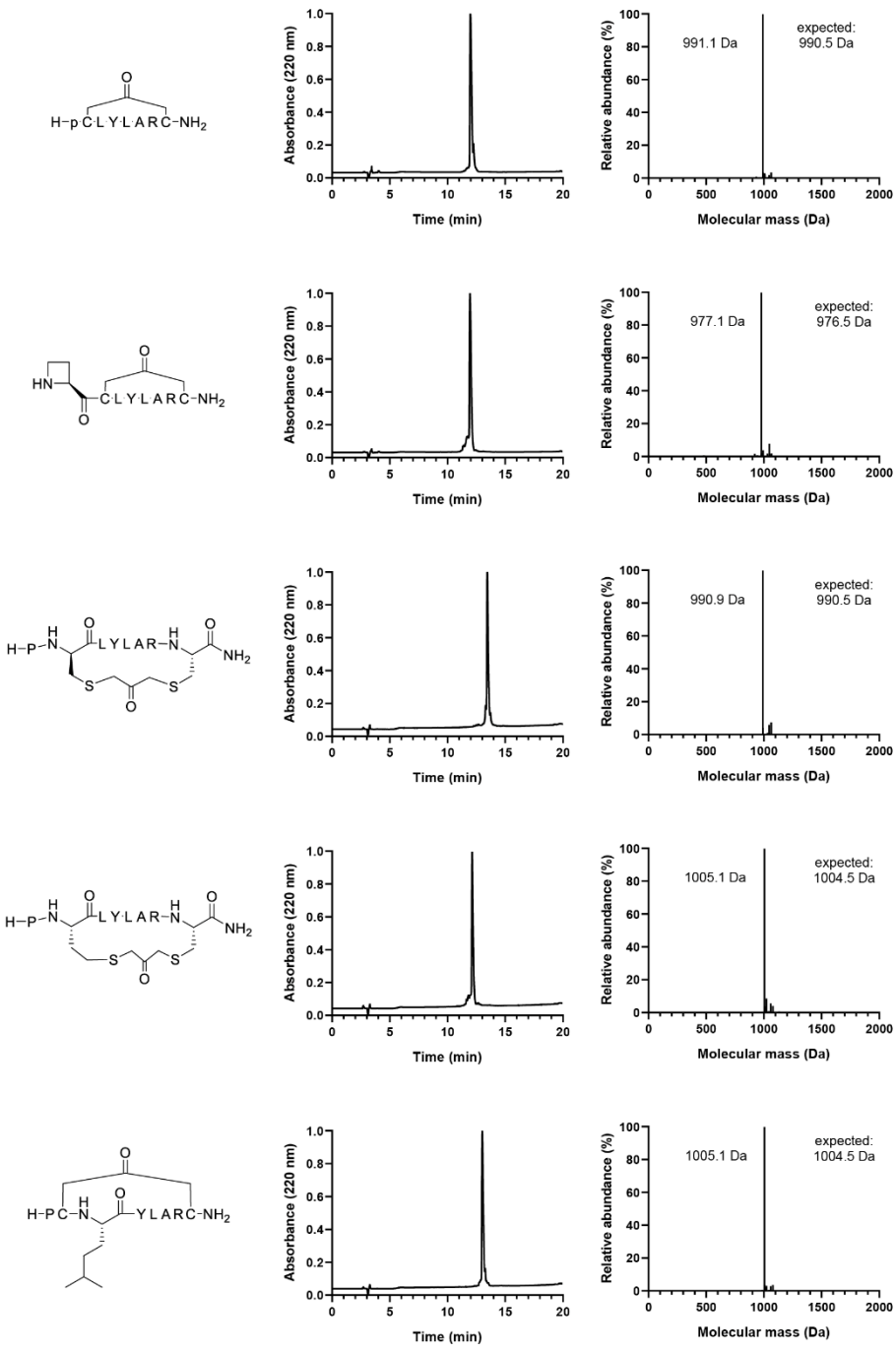

Figure S4. Continued

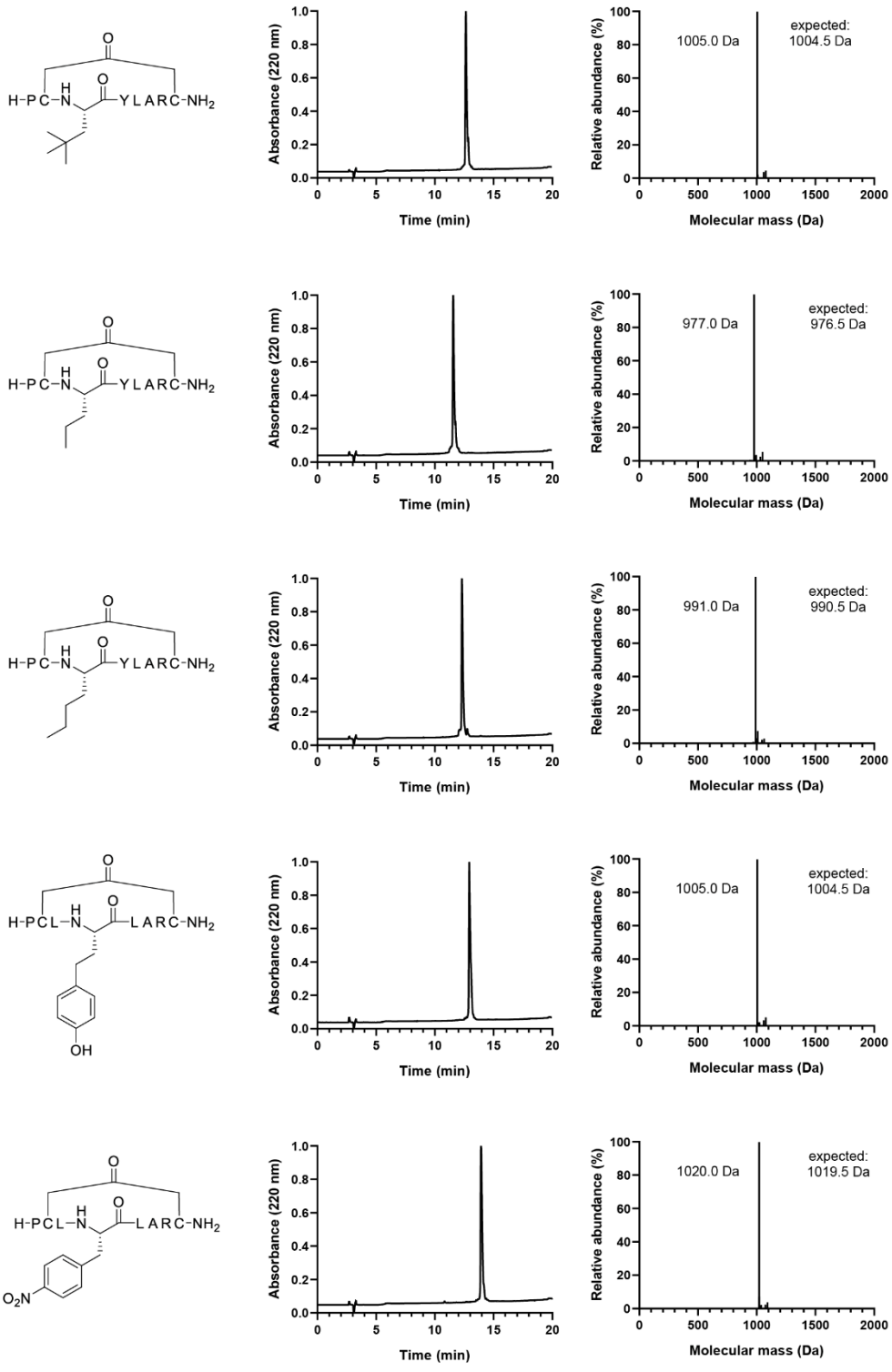

Figure S4. Continued

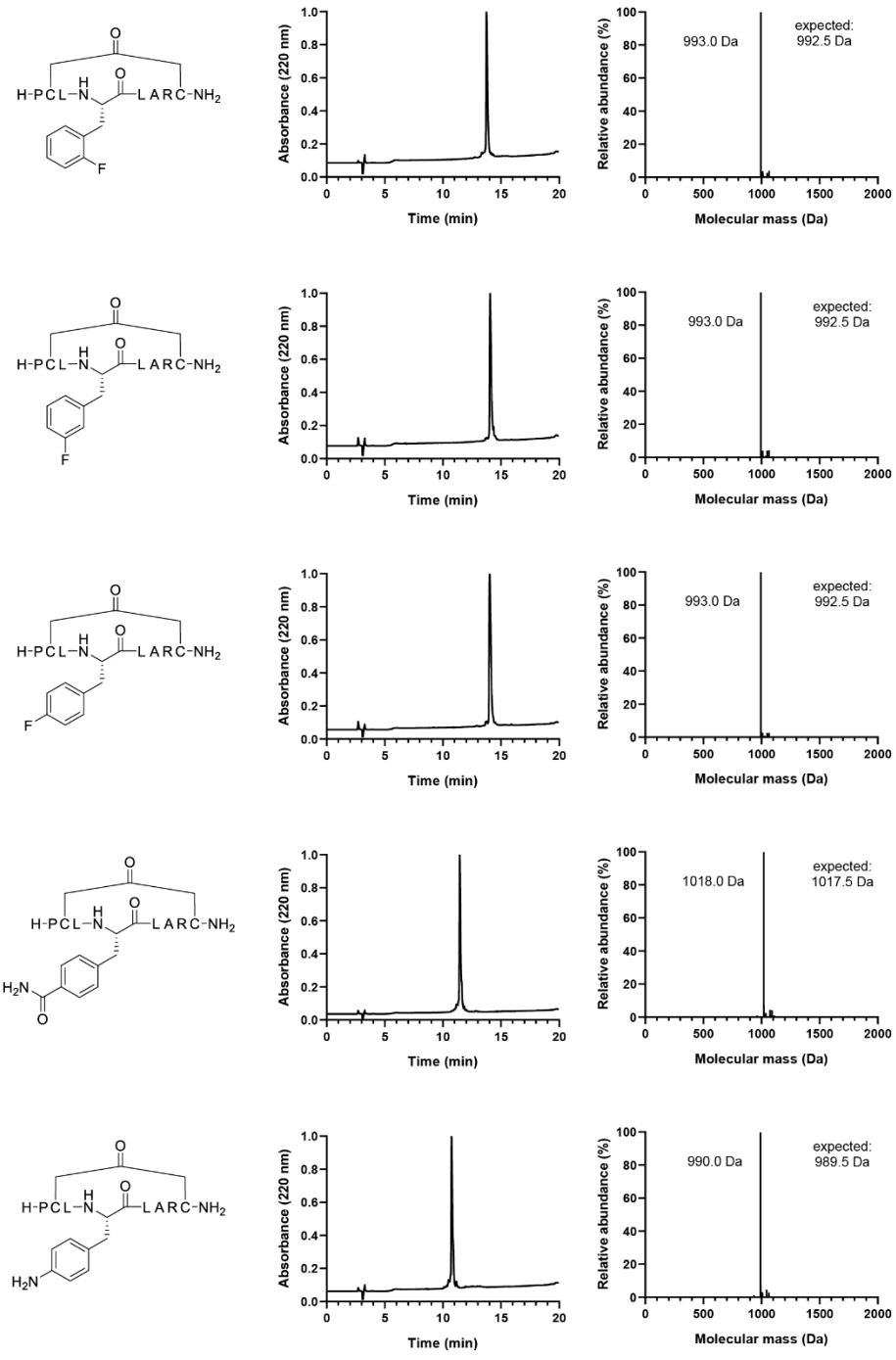

Figure S4. Continued

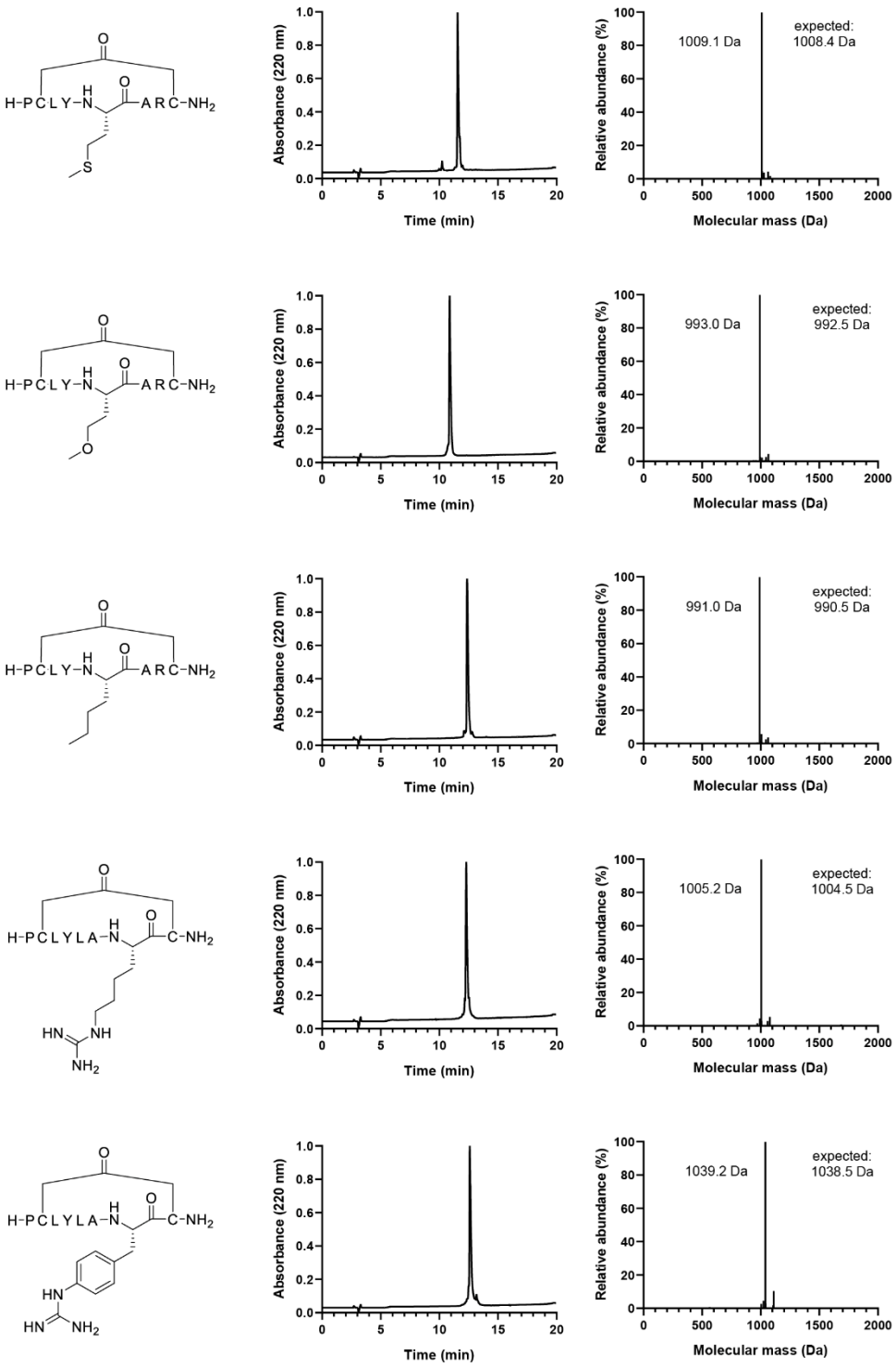

Figure S4. Continued

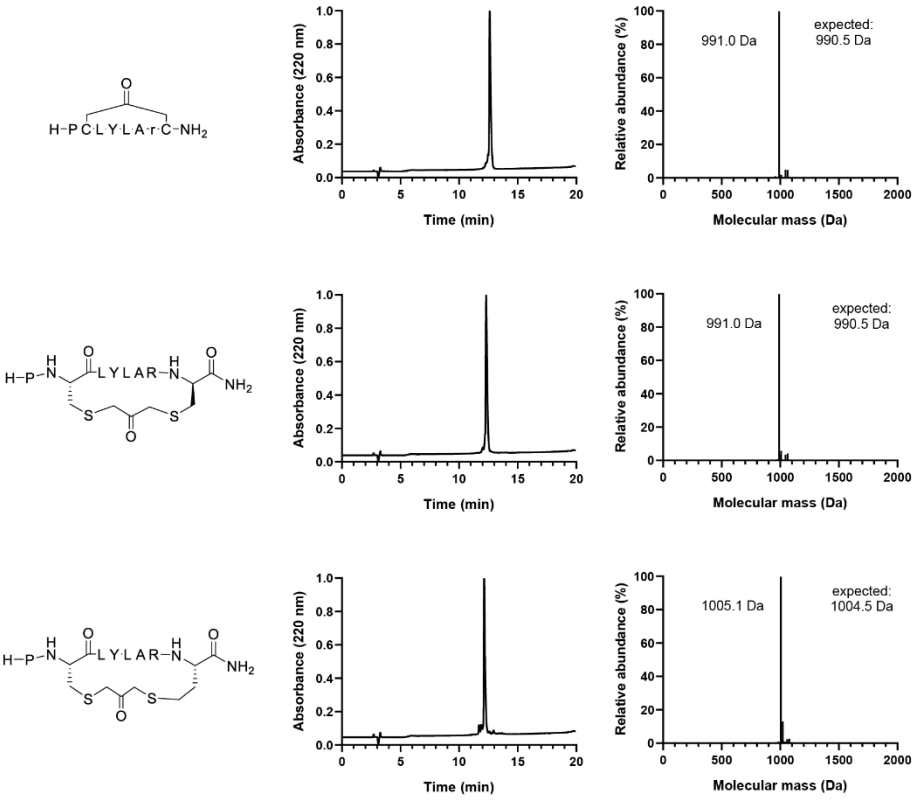

Figure S4. Continued

a

KLK5

	Substitution	K_i (nM) ± SD	fold-change
	KLK5(1)	2.2 ± 0.2	
Gly 1	β-Ala	3.6	1.6
	GABA	4.4	2.0
	Ala	14.0	6.3
	D-Ala	1.4 ± 0.7	0.6
	N-Guanidino-Gly	4.1	1.9
Cys 2	D-Cys	250	115
	HCys	7.8	3.5
Thr 3	Ser	15.8	7.2
	HSer	41	19
	L-allo-Thr	200	91
Arg 4	Lys	32	14.5
	Agb	690	312.7
	Homo-arginine	290	130.7
	4-Guanidino-Phe	32	14.4
5	Cit	2.1	0.9
Tyr 6	HTyr	3.0	1.4
	4-Nitro-Phe	7.0	3.2
	2-Fluoro-Phe	1.6 ± 0.7	0.7
	3-Fluoro-Phe	2.2	1.0
	4-Fluoro-Phe	2.5	1.1
	Cyano-Phe	5.3	2.4
	1-Naphthyl-Ala	2.6	1.2
	2-Naphthyl-Ala	1.4 ± 0.6	0.6
	5-HTTP	4.4 ± 1.4	2.0
Pro 7	D-Pro	138	62.6
	Pip	1.3 ± 0.7	0.6
	D-Pip	59	26.6
	Hyp	2.6	1.2
	β-Pro	19	8.5
	Aze	11.1	5.0
Cys 8	D-Cys	2.2 ± 0.3	1.0
	HCys	8.5	3.9

b

KLK7

	Substitution	K_i (nM) ± SD	fold-change
	KLK7(1) without C-terminal Ser	29 ± 4	
Pro 1	Hyp	162	5.5
	Pip	26	0.9
	β-Pro	44	1.5
	D-Pro	35	1.2
	Aze	135	4.6
Cys 2	D-Cys	840	28.8
	HCys	70	2.4
Leu 3	HLeu	510	17.3
	NptGly	40	1.3
	Nva	109	3.7
	Nle	162	5.5
Tyr 4	HTyr	840	28.8
	4-Nitro-Phe	1550	52.8
	2-Fluoro-Phe	510	17.5
	3-Fluoro-Phe	102	3.5
	4-Fluoro-Phe	260	8.8
	Carbamoyl-Phe	840	28.8
	Amino-Phe	1040	35.5
Leu 5	Met	17.8	0.6
	O-meth-HSer	90	3.1
	Nle	7.0 ± 0.7	0.2
Arg 7	HArg	42	1.4
	4-Guanidino-Phe	34	1.2
	D-Arg	189	6.4
Cys 8	D-Cys	97	3.3
	HCys	40	1.4

c

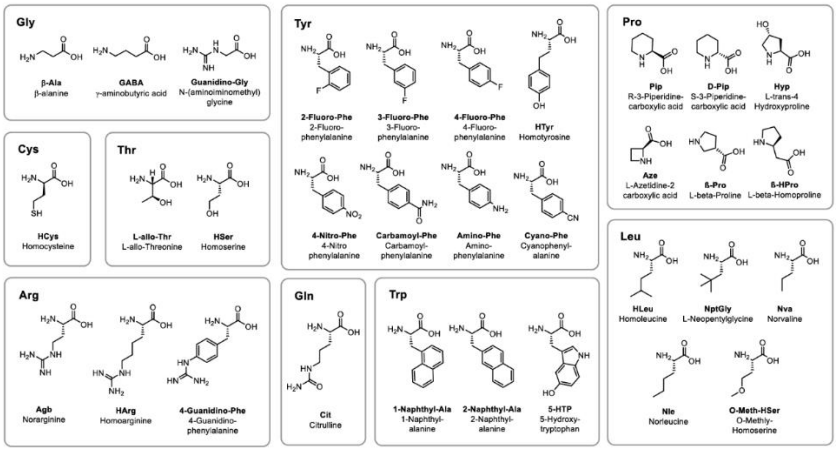

Figure S5. Structure-activity relationship and affinity improvement using unnatural amino acids. a, b, K_i values of variants of the KLK5 inhibiting KLK5(1) (a)

and KLK7 inhibiting KLK7(1) (b). KLK7(1) and its mutants were synthesized without C-terminal serine. For peptides showing improved or nearly unchanged activity, the K_is were measured in two additional experiments, and mean values and SDs are indicated. c, Chemical structures of amino acids used.

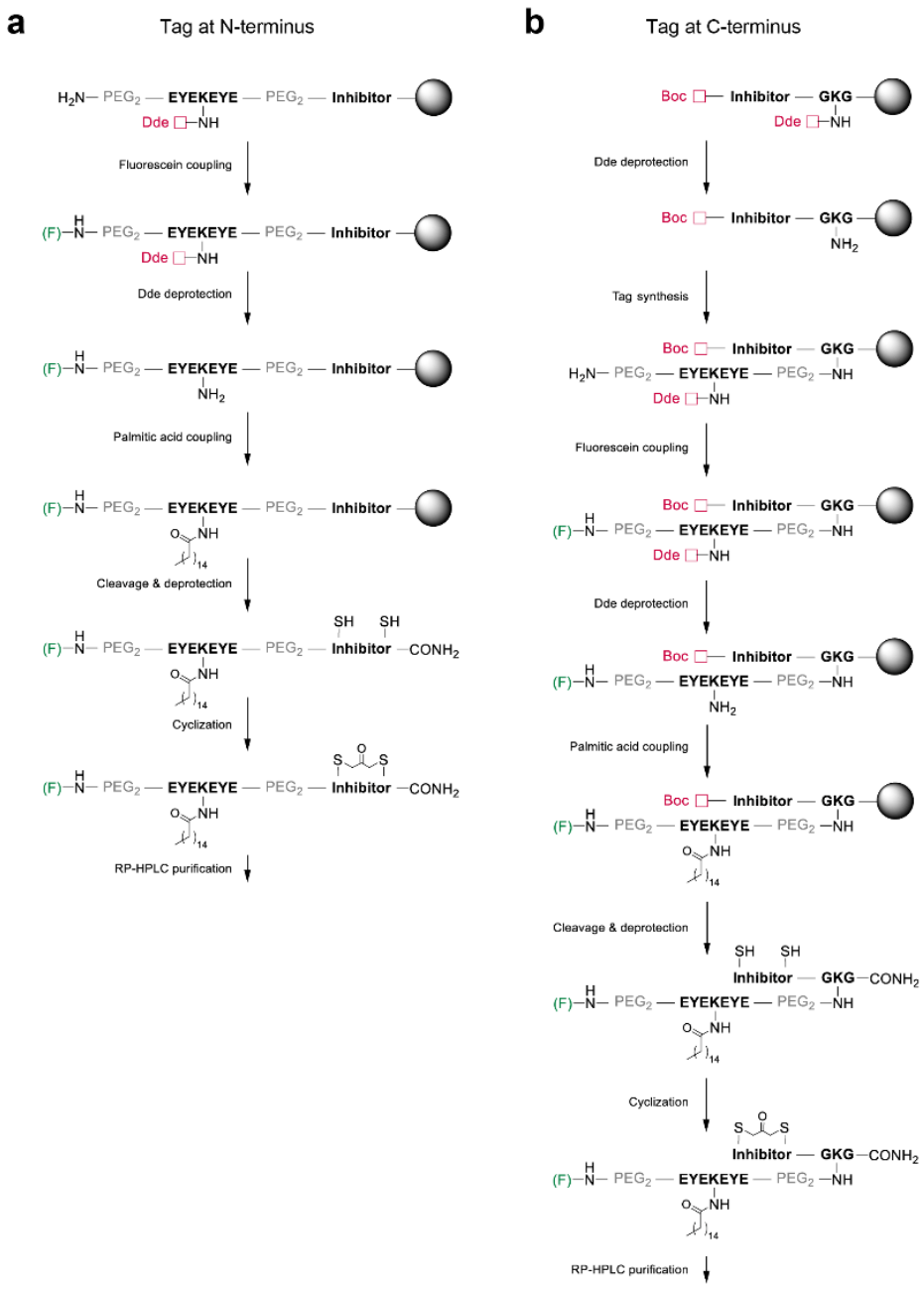

Figure S6. Solid-phase peptide synthesis of conjugates of cyclic peptide KLK inhibitors and albumin tag. a, Synthesis of N-terminal conjugates. After linear synthesis until the N-terminal 5(6)-carboxyfluorescein (F), the side chain of the Lys within the heptapeptide sequence was selectively deprotected and coupled with palmitic acid. After cleavage, cyclization was performed in solution. b, Synthesis of C-

terminal conjugates. The inhibitor was synthesized with a Boc-protected N-terminal amino acid. The side chain of the Lys within the GKG linker was selectively deprotected and the synthesis of the tag continued until 5(6)-carboxyfluorescein (F). In the last step, the side chain of the Lys within the heptapeptide sequence was selectively deprotected and coupled with palmitic acid. After cleavage, cyclization was performed in solution and peptides were purified by RP-HPLC.

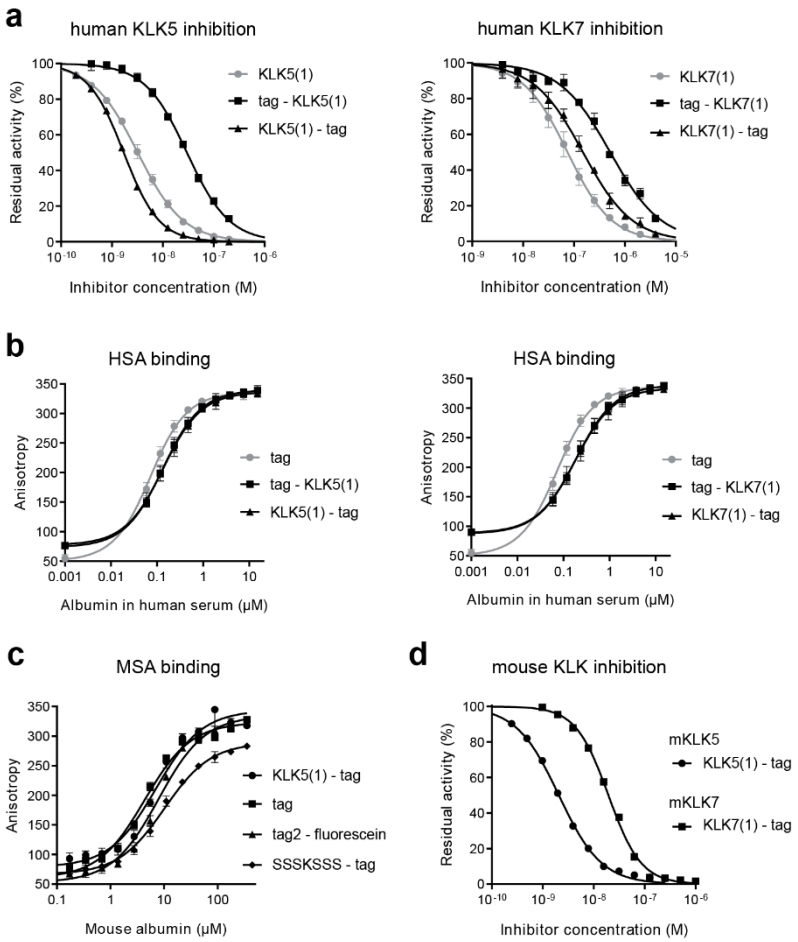

Figure S7. Measurement of KLK inhibition and albumin binding by conjugates. a, Inhibition of human KLK5 (left) and KLK7 (right) by peptides with albumin-binding peptide (tag) conjugated to the peptides' N- or C-terminus. Inhibition was measured in presence of 25 µM human albumin. Mean values and SDs of three independent measurements are shown. b, Binding of conjugates to human serum albumin assessed by fluorescence polarization. Mean values and SDs of three independent measurements are shown. c, Binding of conjugates to mouse serum albumin assessed by fluorescence polarization. The molecule tag2-fluorescein is the tag with the fluorescein group linked to the C-terminus of the heptapeptide. Mean values and SDs of three independent measurements are shown. d, Inhibition of mouse KLK5 and KLK7 by peptide-tag conjugates in presence of 25 µM human albumin.

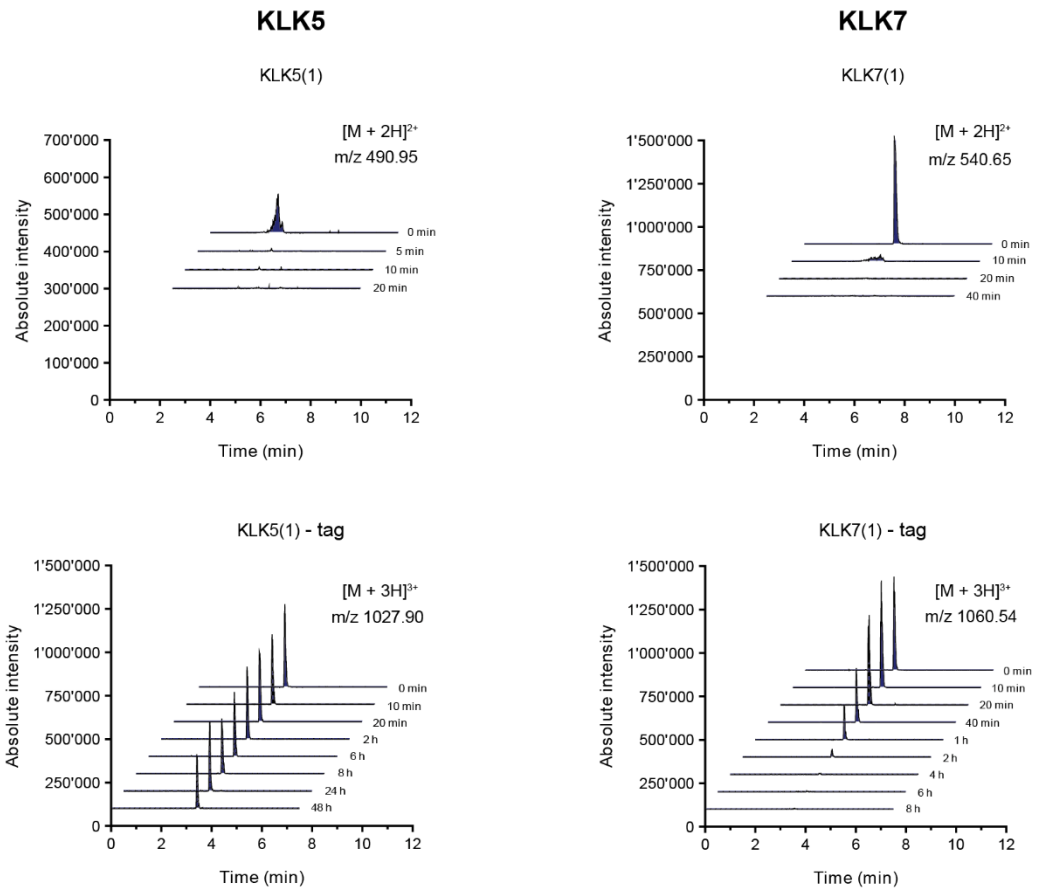

Figure S8. Stability of peptides and peptide conjugates after incubation in human plasma assessed by LC-MS. Peptides and peptide-tag conjugates were incubated at concentrations of 80 μM in human plasma, the plasma proteins removed by precipitation, and the amount of intact peptide quantified by LC-MS. Total ion counts detected for the indicated charged species are shown.

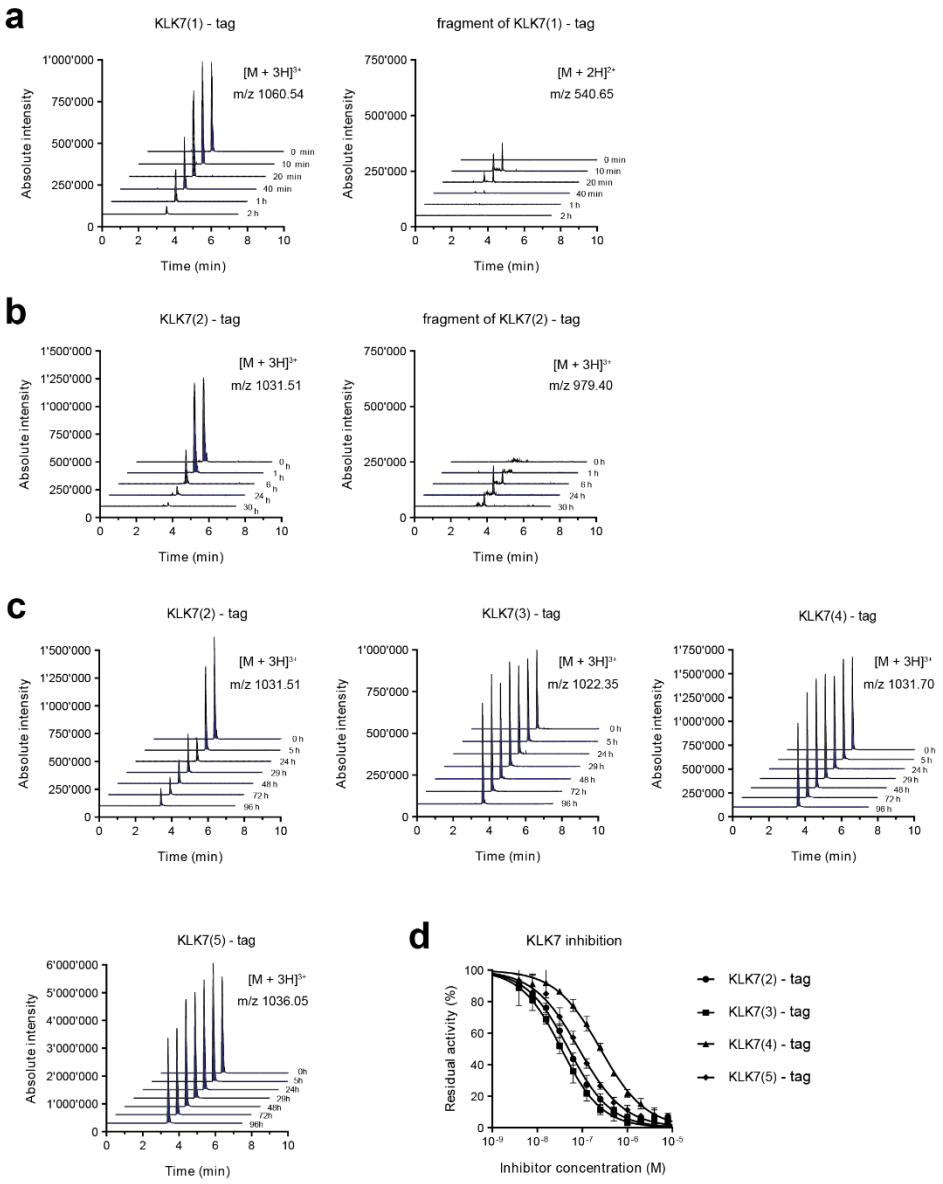

Figure S9. Stability and inhibition activity of KLK7 inhibitor tag conjugates. a-c, Peptide-tag conjugates were incubated at concentrations of 80 μM in human plasma, the plasma proteins removed by precipitation, and the amount of intact peptide quantified by LC-MS. Total ion counts detected for the indicated charged species are shown. d, Inhibition of KLK7 by KLK7(2)-tag and mutants thereof. Mean values and SDs of three independent measurements are shown.

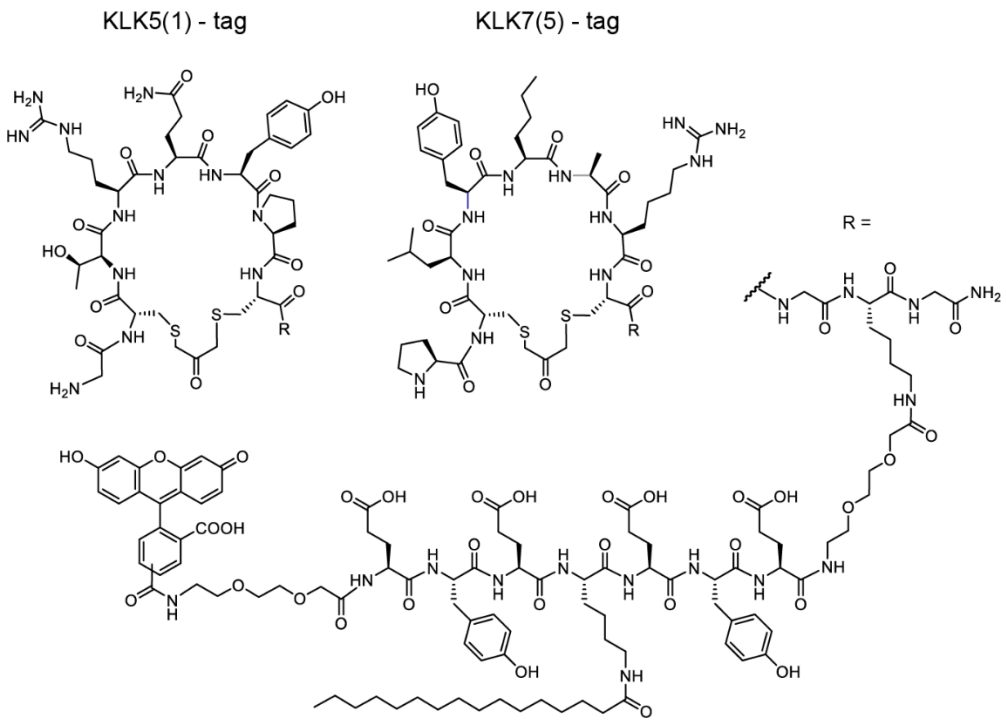

Figure S10. Chemical structures of KLK5(1)-tag and KLK7(5)-tag.

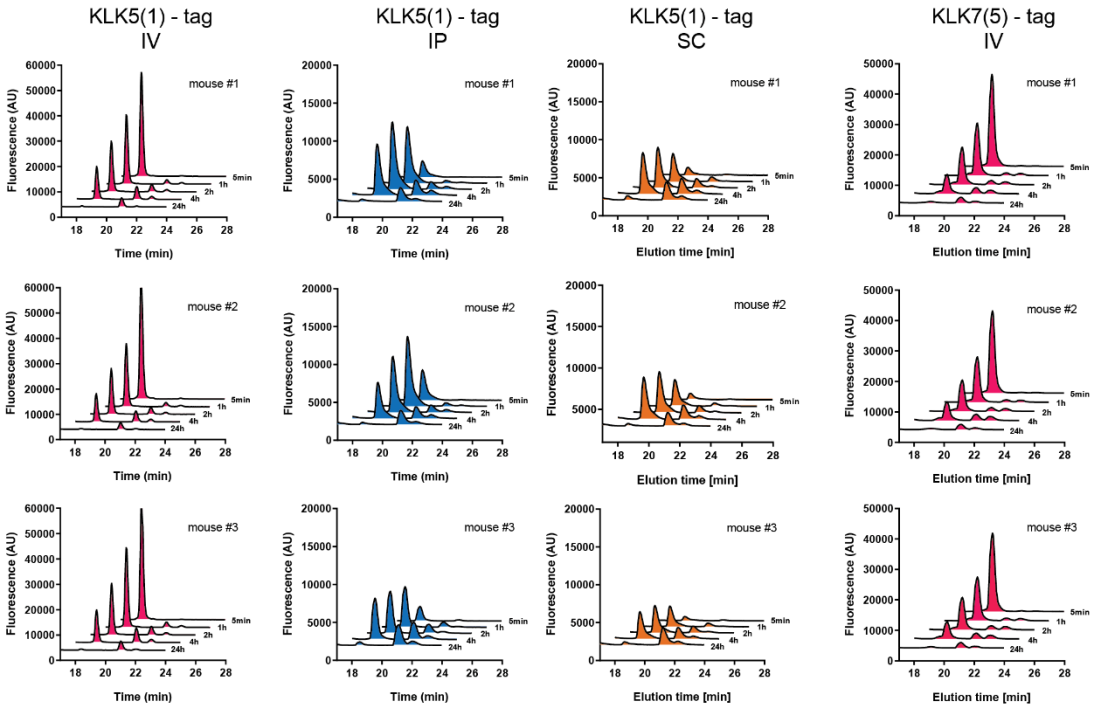

Figure S11. RP-HPLC analysis of KLK inhibitor conjugates in blood samples taken from mice at different time points after administration. KLK5(1)-tag and KLK7(5)-tag were applied to groups of three mice, blood samples taken at the indicated time points, and fluorescent species analyzed by RP-HPLC using a fluorescence detector. Application routes: intravenous (IV), intraperitoneal (IP) and subcutaneous (SC).

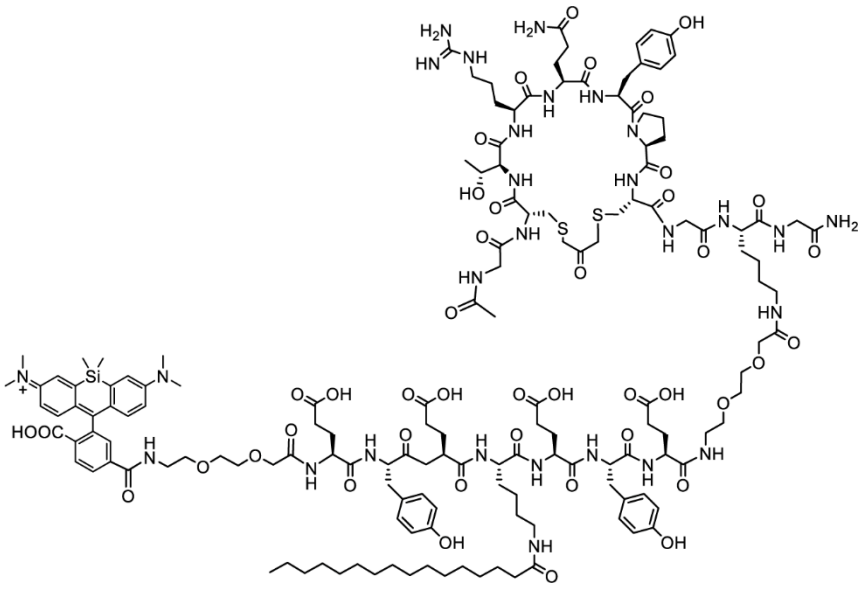

Figure S12. Chemical structure of KLK5(1)-SiR-tag.

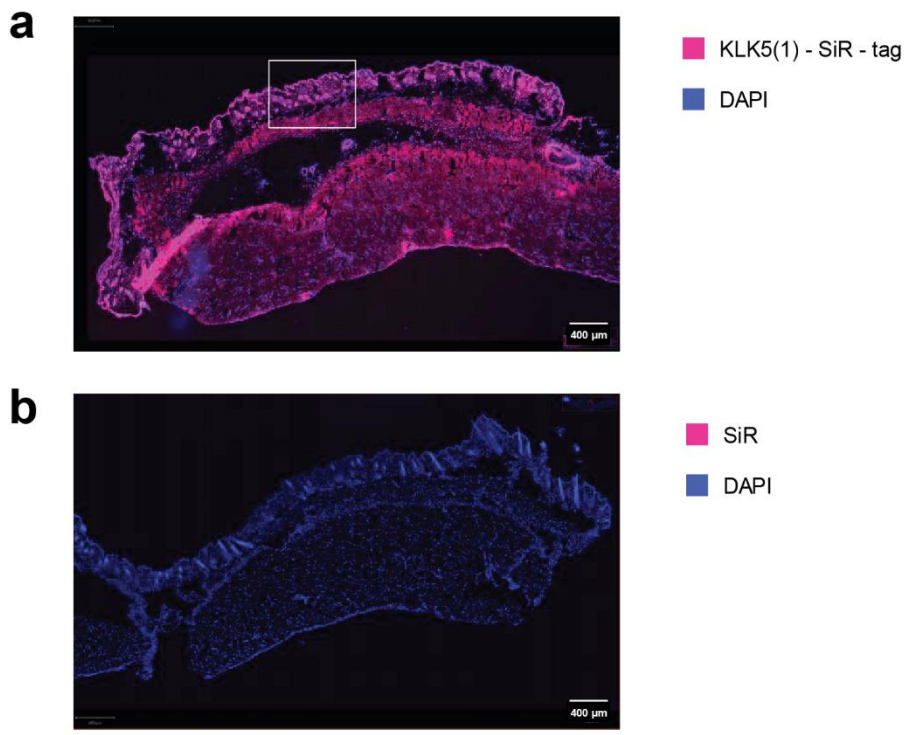

Figure S13. Distribution of KLK5(1)-SiR-tag and fluorophore alone (SiR) in mouse skin. Mice were injected with KLK5(1)-SiR-tag (6.4 mg/kg; 2 µmol/kg; n = 1) or SiR (1 mg/kg; 2 µmol/kg; n = 1), sacrificed after eight hours, and skin sections analyzed by fluorescence microscopy. The SiR-tag is the same albumin-binding molecule as the tag, but with SiR instead of fluorescein as the fluorophore. SiR is excited and emits at a longer wavelength at which less background fluorescence from tissue occurs. Fluorescence is shown in red and DAPI (cell nuclei) in blue.